EFFECTIVENESS OF WIDELY USED CRITICAL VELOCITY AND BED SHEAR STRESS EQUATIONS FOR DIFFERENT TYPES OF SEDIMENT BEDS

By

S. M. HELALUR RASHID

A thesis submitted in partial fulfillment of
the requirements for the degree of

MASTER OF SCIENCE IN CIVIL ENGINEERING

WASHINGTON STATE UNIVERSITY
Department of Civil and Environmental Engineering

DECEMBER 2010

To the Faculty of Washington State University:

The members of the Committee appointed to examine the thesis of S. M. HELALUR RASHID find it satisfactory and recommend that it be accepted.

_____

Michael E. Barber, Ph.D., Chair

_____

Akram Hossain, Ph.D.

_____

Cara Poor, Ph.D.

Acknowledgements

Firstly, I would like to thank my advisor, Dr. Michael Barber, for giving me the opportunity to work in this project and providing great enthusiasm, guidance and support throughout my stay. He had taught me so much, allowed me the freedom to pursue my own ideas, and pointed out when I was off track. I would like to thank Dr. Akram Hossain for his encouragement and support to get into the MS program at WSU. I would also like to thank my committee, Dr. Cara Poor for all the useful comments she provided. I am very grateful for the support the Department of Energy (DOE) and the Energy Solutions (ES) gave for this research. Special thanks to Mark Siegenthaler for his helpful comments and thought-provoking discussions from the very beginning of my research.

Thanks to Nazmul, Zhumur, Barik, Solaiman, and Josh for being always with me as friends and roommates to make this journey a memorable one. I would like to thank my colleagues, Travis, Matt, Lisa, Kirsti, Nick, Wes, and Josh for making this project a successful one.

Finally, I would like to thank my parents, who have always been encouraging and supportive of my aspirations. In so many ways, they managed to make everything so much easier for me.

EFFECTIVENESS OF WIDELY USED CRITICAL VELOCITY AND BED SHEAR STRESS EQUATIONS FOR DIFFERENT TYPES OF SEDIMENT BED

Abstract

By S. M. HELALUR RASHID, M.Sc.
Washington State University
DECEMBER 2010

Chair: Michael E. Barber

Critical bed shear stress and velocity estimations of sediment particles are the two fundamental properties that help to understand sediment transport, scour, and deposition under different flow conditions. Six widely used bed shear estimation methods (i.e., Shields, Log Profile (LP), Prandtl's Seventh Power (PSP), Turbulent Kinetic Energy (TKE), Reynolds Stress (RS), and Kim et al. 2000) were compared using flume study. Two widely used sediment transport rate estimation methods (i.e., Ackers and White, and Engelund and Hansen) were applied for known sediment transport rates for calculating bed shear stresses and then compared with bed shear stress estimation methods. An Acoustic Doppler Velocimeter (ADV) for velocity and turbulence measurements and a Laser Displacement Meter (LDM) for sediment transport rate measurements were used in a re-circulating, low turbulence linear flume (3.66 m (12 ft) long, 0.884 m (2.9 ft) wide and 0.61 m (2.0 ft) deep). A consistent log layer of 2.0 cm was found for all the experiments. Velocity data 0.4 cm above the sediment bed which was the closest possible accurate velocity measuring points to the sediment bed was used for the turbulence

analysis based bed shear estimation methods. RS method showed good agreement with the TKE (Slope = 0.779, R^2 = 0.788) and LP methods (Slope = 0.773, R^2 = 0.861) for sediment beds with uniform sands. The Shields and Kim et al. (2000) methods estimated very low critical bed shear stresses and the PSP method estimated the highest critical bed shear stresses for sediment bed with uniform sands. The bed shear stress estimated from Engelund and Hansen's method showed considerable agreement with the TKE and RS methods and Ackers and White's method showed large discrepancies with all the bed shear estimation methods for the existing flow condition. Experiments performed with sand mixture sediment beds showed very interesting results. Sediment beds with different sizes of sand particles tended to develop a bed shear stress similar to sediment beds with the dominant particle size in the mixed sediment beds. Moreover, discrepancies among the bed shear stress estimation equations were higher for sediment beds prepared by different particle sizes. Different bed shear estimation methods compared in this study using advanced velocity and sediment transport rate measuring instruments will add confidence to previous and current research.

Table of Contents

Acknowledgements iii

Abstract iv

List of Tables viii

List of Figures ix

Chapter 1: Introduction 1

Chapter 2: Background 6

2.1. Sediment transport rate 7

2.1.1. Ackers and White's formula 8

2.1.2. Engelund and Hansen's formula 9

2.2. Bed shear stress estimation methods 10

2.2.1. Log Profile (LP) method 10

2.2.2. Average shear velocity method 11

2.2.3. Quadratic stress law method 11

2.2.4. Reynolds stress or Covariance (COV) method 12

2.2.5. Turbulent Kinetic Energy (TKE) method 12

2.2.6. Prandtl's seventh power (PSP) law 13

Chapter 3: Methodology 15

3.1. Acoustic Doppler Velocimeter (ADV) 16

3.2. Calibration of ADV 20

3.3. Laser Distance Meter (LDM) 21

3.4. Preparation of sediment bed 22

Chapter 4: Results 25

4.1. Comparison among the bed shear stress estimation methods 25

4.2. Relationship between critical bed shear stress and average flow velocity 29

4.3. Comparison of bed shear stress estimation methods with sediment transport rate estimation approaches 30

4.4. Comparison of critical bed shear stress between different sizes of sediment beds and sediment mixture beds 34

4.5. Importance of selecting velocity data point for the turbulence based bed shear stress methods 37

Chapter 5: Discussions 39

Chapter 6: Conclusions 44

Reference List 47

Appendix 1 51

List of Tables

Table 3.1 Physical test sand properties. 23

Table 3.2 Configuration of sediment mixture. 23

Table 4.1 Critical bed shear stress for different sizes of sand particles 26

Table 4.2 Comparing the bed shear stress estimation equations with sediment transport estimation approaches. 32

Table 4.3 Critical bed shear stresses for different sizes of sediment beds and different mixtures of sediment beds. 34

List of Figures

Figure 3. 1 Schematic of linear low-turbulence flume. 15

Figure 3. 2 Nortek ADV probe with transducer, receiver, and sampling volume (Reproduced with permission from Nortek-US). 17

Figure 3. 3 Relationship between percent change in velocities and signal correlation. 19

Figure 3. 4 A complete test set up showing ADV, Drive motor, LDM, and sediment bed. 24

Figure 4. 1 Critical bed shear stress estimated from five different methods for different sand particle sizes. 27

Figure 4. 2 Comparison of Reynolds stress with LP, TKE, and Kim et al. methods. 28

Figure 4. 3 Relationship between critical bed shear stress and average flow velocity. 29

Figure 4. 4 Change in sediment bed elevation for type C sand measured by LDM. 30

Figure 4. 5 Sediment bed Plan views for the type C and D sands. 31

Figure 4. 6 Comparison of pseudo measured value with LP, TKE, Reynolds and Kim et al. methods. 33

Figure 4. 7 Comparison of critical bed shear stress of type A and type C sands with sediment mixtures prepared using different percentages type A and type C sands. 36

Figure 4. 8 Comparison of critical bed shear stress of type B and type D sands with sediment mixtures prepared using different percentages type B and type D sands. 37

Chapter 1: Introduction

Sediment scour and transport play very important roles both in natural systems such as rivers and estuaries and in industrial applications such as the US Department of Energy's Hanford Radioactive Waste Pretreatment and Vitrification Plant (HRWPVP). Understanding sediment supply, scour, transport, and deposition in natural channels and watersheds can help establish practices to minimize field erosion and channel degradation in order to maintain stream ecology, minimize reservoir sedimentation and dredging requirements, and control fate and transport of sediment-bound contaminants (Wilcock 2001; Cui and Parker 2005; Lamb et al. 2008). Furthermore, improved estimation of critical shear stresses (or entrainment velocity) for different sediments (type, size, and density) is critical to improving parameterization of numerical simulation models developed for predicting deposition, resuspension, and mixing in waste treatment facilities such as the radioactive sediment vessels in the HRWPVP.

The complex combination of forces acting on a sediment particle along with particle characteristics, fluid properties, and channel characteristics make the study of sediment scour and transport parameters a very challenging subject with local data sometimes supporting different conclusions. For example, in cohesionless soils, it is widely believed that critical bed shear stress decreases as bed slope increases due to increased gravitational force in the direction of flow (Wiberg and Smith 1987; Lau and Engel 1999; Molinas and Wu 2001; Aksoy and Kavvas 2005). However, for model simplicity, most bed load transport models ignore the influence of channel slope on the sediment transport rate which is not true for mountainous rivers with steep slopes (Lamb et al. 2008). In fact, in their study, Lamb et al. (2008) found that critical bed shear stress actually increases with increases in bed slope.

Furthermore, incipient motion of a particle in a sediment bed depends on the particle's physical size, shape, density, angle of repose or armored bed, and protrusion of the particle into the flow (Wiberg and Smith 1987). But, Wilcock and Southard (1988) and Shvidchenko et al. (2001) found that critical bed shear stress was independent of the well sorted or poorly sorted sediment mixtures. Recently, Wilcock and Crowe (2003) developed a transport model which showed that sediment transport rate should be a function of bed-surface particle sizes instead of median particle size of total sediment bed. Substantial disagreement among the researchers for defining the dominant forces and parameters on the particle movement is a major reason for the continuation of similar studies.

Sediment transport parameters have been broadly studied by a large number of researchers (Prandtl 1926; Hjulstrom 1935; Shields 1936; White 1940; Einstein 1950; Meyer-Peter and Muller 1977; Yang 1979; Parker and Klingelman 1982; Komar 1987; Wilcock 1993; Papanicolaou 2001) over the past eight decades. A large number of different equations have been proposed for predicting critical velocity and bed shear stress. Most of these equations for predicting critical velocity and bed shear stress rely on indirect methods (i.e. estimating shear stress using other measured parameters), which affect the accuracy of these equations (Wilcock 1996; Papanicolaou et al. 2002; Pope et al. 2006) or single grain sizes which limit extrapolation to mixed (real) grain size distributions (Wilberg and Smith 1987; Wilcock and Southard 1988; Kuhnle 1993). Moreover, precise flow velocity measurements at different locations in the channel are very important for successful application of these equations. However, some direct measurement methods of bed shear stress such as skin friction probes (Gust 1988), Preston tubes (Nezu and Nakagawa 1993; Krishnappan and Engel 2004), flow deceleration, and numerical simulation (Thompson et al. 2003), Prandtl-Pitot tubes (Ahmed and Rajaratnam 1998), and shear

plates (Rankin and Hires 2000; Barnes et al. 2009; You and Yin 2007) have been used in laboratory flumes. Nevertheless, difficulties in implementing these direct measurement techniques in field environments along with relatively low confidence in the accuracy of the direct measurements still restrict their use primarily to laboratory flumes (Rankin and Hires 2000; Biron et al. 2004; Rowinski et al. 2005).

Recently, there have been many technological developments concerning the accuracy of flow velocity measurements; specially, flow velocities near sediment beds. The invention and adoption of Electromagnetic Current Meters (EMCM), Laser Doppler Velocimeters (LDV), Acoustic Doppler Current Profilers (ADCP), and Acoustic Doppler Velocimeters (ADV) for flow measurement call for a thorough re-evaluation of the widely used critical velocity and bed shear stress equations. Because bed shear stress estimation methods were mostly developed using flume studies and measurements of parameters (e.g., velocity, velocity fluctuations, near bed turbulence) were subject to measuring errors, improvement of bed shear stress estimation methods can be made by reducing these errors using recently developed technologies. These advanced velocity measuring instruments have already been used by number of researchers (e.g., Kim et al. 2000; Biron et al. 2004; Thompson et al. 2003; Rowinski et al. 2005; Pope et al. 2006) in bed shear stress estimation studies. The study of evaluating widely used critical velocity and bed shear stress estimation methods will be helpful to boost confidence in ongoing research.

The objectives of this study were to use advanced measurement technologies to investigate the following aspects of six widely used critical velocity and shear stress equations:

1. Compare the shear stresses estimated by Log-profile (LP), Prandtl's Seventh Power (PSP) law, Turbulent Kinetic Energy (TKE), Reynolds stress (RS) method, and

equation proposed by Kim et al. (2000) under different sediment beds with the help of precise point velocity and turbulence measurements.

2. Estimate shear stress from the measured sediment transport rates using the widely accepted Ackers and White (1973) and Engelund and Hansen (1967) sediment transport equations. In addition, compare and contrast these shear stresses to predictions using the LP, PSP, TKE, RS, and Kim et al. (2000) methods.
3. Compare and contrast shear stresses for sediment beds with mixtures of sand sizes compared to sediment beds with uniform sand sizes present in the mixture.

In the past, investigation of critical bed shear stress equations were mostly performed under uniform sediment beds (Shields 1936; White 1940; Vanoni 1964; Yalin and Karahan 1979; Buffington and Montgomery 1997; Thompson et al. 2003; Biron et al. 2004). While these studies were often repeated using several different sand sizes for comparison, few actually combined grain sizes to determine the combined impacts. Furthermore, many early flume studies were performed with pitot tubes, micropropellers, or some other less accurate velocity measurement device and actual sediment scour rates were relatively subjective (Shields 1936; White 1940; Vanoni 1964; Yalin and Karahan 1979; Wiberg and Smith 1987; Wilcock and Southard 1988; Shvidchenko et al. 2001). In this study, we used a wide range of sand particles to verify whether the effectiveness remain similar for different particle sizes with the help of advanced velocity and turbulence measuring instrument (ADV). Moreover, sediment beds with mixture of sands were used to understand how the mixing proportion of different sediment sizes influence the bed shear stresses. Sediment transport and bed shear stress were correlated in different sediment transport rate equations calibrated using laser distance measurements. Bed shear stresses were estimated from the measured sediment transport rate using the sediment transport rate equations.

A better comparison of bed shear stress estimation equations would be possible using this new approach. In addition, the compatibility of different bed shear stress estimation and sediment transport rate equations under different flow conditions could be analyzed.

Chapter 2: Background

As flow velocity over a stationary cohesionless sediment bed in a channel or stream increases, a threshold will occur at which the forces holding the particles in place will no longer be able to resist the hydrodynamic forces (i.e. drag, lift, gravity, collision of particles) acting upon them. As a result of this failure to resist the hydrodynamic forces, the particle will start to move. The transition from a state of "no motion" to the "initiation of motion" is defined as the critical condition of incipient motion, and related to the first stage of sediment transport (Paphitis 2001; Beheshti and Ataie-Ashtiani 2008). Initiation of motion can occur by rolling, sliding, lifting, bouncing or impact ejection of particles from a stationary sediment bed (Yang 1977; Mehta and Lee 1994; Ling 1995). Incipient motion criteria can be obtained by solving the forces acting on the stationary particle (Yang 1977; Ling 1995; Wu and Chou 2003). Theories developed for bed shear velocity and bed shear stress estimation are based on specific assumptions such as flow condition (e.g. laminar/turbulent flow, depth of water etc.), particle size of bed load, velocity distribution, and channel roughness (Kim et al. 2000).

The approaches for developing these theories can be grouped into three categories: (1) first-order moment statistics methods (mean)including the log profile (LP) method, average shear velocity method and quadratic stress law method; (2) second-order moment statistics (variance) including the Turbulent Kinetic Energy (TKE) method or Covariance (COV) method (also known as Reynolds stress method); and (3) spectral analysis methods such as the Inertial Dissipation (ID) method (Kim et al. 2000; Pope et al. 2006; Westenbroek, 2006). Most of the bed shear stress estimation theories consider channel velocity as a vector, having three components in a Cartesian coordinate (x, y, z) system (Kim et al. 2000; Biron et al. 2004). A velocity vector **u** =

(u, v, w) is defined with u acting in the mean flow direction x, v acting horizontally across the mean flow direction y, and w acting vertically across the mean flow direction z. Various bed shear velocity and bed shear stress estimation methods have been widely used over the years because of their simplicity, ease of parameter measurements, and accuracy in a wide range of flow conditions. Some widely used and advanced bed shear velocity and bed shear stress estimation methods will be further described below. Many current researchers (e.g., Wolf 1999; Kim et al. 2000; Thompson et al. 2003; Biron et al. 2004; Rowinski et al. 2005; Westenbroek 2006; Pope et al. 2006) have considered these bed shear estimation methods in their studies.

2.1. Sediment transport rate

Sediment transport rate in a fluvial channel can be estimated using the empirical formula developed from flume studies, using a trap or settling pond to catch the sediment, or tracking sediment movement using instrumentation such as an Acoustic Doppler Current Profiler (ADCP) or a Laser Displacement Meter (LDM) (Molinas and Wu 2001; Wilcock 2001).

We used both the Ackers and White's sediment transport rate formula and the Engelund and Hansen's sediment transport rate formula to calculate bed shear stress from the known sediment transport rate. These two equations were chosen because of their applicability to a wide range of flow conditions, and availability of the required parameter measurements with our experimental setup. Moreover, these equations were widely used by researchers to estimate sediment transport rate and compare these equations with others (Molinas and Wu 2001; Bisantino et al. 2010). Ackers and White and Engelund and Hansen sediment transport rate formulas are described below.

2.1.1. Ackers and White's formula

Based on Bagnold's stream power concept (1966) and the mobility theory, Ackers and White (1973) developed their transport function using dimensional analysis. Bagnold (1966) defined stream power concept as "the available power supply, or time rate of energy supply, to unit length of a stream is clearly the time rate of liberation in kinetic form of the liquid's potential energy as it descends the gravity slope". The available stream power supply can be expressed as:

$$\Omega = \rho g Q S \quad (1)$$

where ρ is the density (kg/m^3) of water, g is the gravitational acceleration (m/s^2), Q is the discharge (m^3/s) of the stream, and S is the gravity slope (m/m).

The mobility number can be defined as the ratio of the shear force on unit area of the bed to the immersed weight of a layer of grains (Ackers and White 1973). Ackers and White (1973) assumed that coarse sediments are transported by a portion of total shear stress, and fine sediments are transported by the total shear stress acting in the system. The sediment mobility number can be expressed as:

$$F_{gr} = U_*^n \left[gd\left(\frac{\gamma_s}{\gamma} - 1\right)\right]^{-\frac{1}{2}} \left[\frac{V}{\sqrt{32}\log\left(\frac{\alpha D}{d}\right)}\right]^{1-n} \quad (2)$$

where U_* is the shear velocity (m/s), n is the transition exponent which depends on the sediment size, α is a coefficient in rough turbulent equation, d is the sediment particle size, D is the water depth (m) in the stream, d is the sediment particle size (m), and γ_s and γ are the specific weight (N/m^3) of particle and water respectively.

Sediment transport rate in terms of mass flow per unit mass flow rate can be calculated using the following equation.

$$X = \frac{G_{gr}\, d\gamma_s/\gamma}{D(\frac{U_*}{V})^n} \quad (3)$$

where $G_{gr} = C(\frac{Fgr}{A} - 1)^m$, which is a general dimensionless sediment transport function. A, C, and m are coefficients. Ackers and White obtained their dimensionless parameters A, C, m, and n from 925 flume experiments where they used particles range from 0.04 mm to 4.0 mm and a flow depth of 0.4 m (1.31 ft).

2.1.2. Engelund and Hansen's formula

Engelund and Hansen (1967) developed their sediment transport formula using Bagnold's stream power concept (1966) and the similarity principle. The principle of similarity can be defined as a system of non-dimensional parameters which is obtained to characterize the flow system. The characteristics of a flow system include geometry, kinematic, and dynamic. They used 116 flume experiment data performed by Guy et al. (1966) to obtain their sediment transport formula. Guy et al. (1966) used particle sizes of 0.19, 0.27, 0.45, and 0.93 mm with a flow depth up to 0.34 m for all of their experiments. Engelund and Hansen found that their equation can be applied to a dune bed and the upper flow regime with particle size greater than 0.15mm without serious deviation from the theory. The equation for the sediment transport rate developed by Engelund and Hansen (1967) can be written as:

$$q_s = 0.05\gamma_s V^2 [\frac{d_{50}}{g(\frac{\gamma_s}{\gamma} - 1)}]^{0.5} [\frac{\tau_0}{(\gamma_s - \gamma)d_{50}}]^{1.5} \quad (4)$$

where d_{50} is the median sediment particle size (m) and τ_0 is the bed shear stress (N/m^2).

2.2. Bed shear stress estimation methods

2.2.1. Log Profile (LP) method

Under neutrally stratified, horizontally homogenous, and steady flow conditions, velocity variation above the sediment bed is often estimated using a log profile (Wilcock 1996; Kim et al. 2000). The log profile (LP) equation is commonly known as the von Karman-Prandtl law of vertical velocity distribution equation and can be written as:

$$\frac{u}{u_*} = \frac{1}{K} \ln\left(\frac{z}{z_0}\right) \quad (5)$$

where u is the flow velocity at height z above sediment bed (m/s) , u_* is the bed shear or friction velocity (m/s), K is the von Karman constant (K = 0.4), and z_0 is the roughness height (m) where velocity is assumed to be zero. Bed shear stress can be calculated from:

$$\tau_0 = \rho u_*^2 \quad (6)$$

where $\tau_0$is the bed shear stress (N/m^2), and ρ is the density (kg/m^3) of flowing water.

Depending on the flow condition, the log-layer depth will be different. Bathurst (1982), Nezu and Nakagawa (1993), and Bridge and Jarvis (1976) suggested 20 percent of the flow depth as the log-layer depth, while Bridge and Jarvis (1977) suggested 15 percent and Ferguson et al. (1989) suggested over 50 percent of the flow depth as the log-layer depth. Moreover, in a shallow water environment, number of available velocity data may not be enough to get an acceptable log profile. Biron et al. (1998) showed that number of velocity data within the log-layer and altercation of the log-layer depth both result in very different shear stress estimates. Uncertainties in establishing a log velocity profile under different flow conditions affect the accuracy of this widely used method (Wilcock 1996; Williams 1995; Biron et al. 1998; Babaeyan-Koopaei et al. 2002).

2.2.2. Average shear velocity method

An average bed shear velocity of a reach can be calculated by a general force balance approach as:

$$u_* = \sqrt{gRS_f} \quad (7)$$

where g is the gravitational acceleration (m/s^2), R is the hydraulic radius (m), and S_f is the energy slope (m/m). Bed shear stress can easily be calculated by using the average bed shear velocity (u_*) in Equation 6. This method might not be suitable for local, small-scale estimates of the variations in shear stress due to the larger length requirement for the measurement of the energy slope (Babaeyan-Koopaei et al. 2002; Biron et al. 2004). Moreover, precise energy slope measurement is not always possible which eventually affects the accuracy of the method. For most of the cases, it is assumed that energy slope is equal to the bed slope which is necessarily not true in all flow conditions.

2.2.3. Quadratic stress law method

The quadratic stress law relates average bed shear stress to depth-averaged flow (Williams, 1995) and can be written as:

$$\tau_0 = \rho C_d u^2 \quad (8)$$

where C_d is the single, integrated depth-average and spatially-averaged drag coefficient, and u is the depth averaged velocity (m/s) in the direction of flow.

Drag coefficient is not a constant and in practice, a constant value of C_d is used which is independent of flow speed (Thompson et al. 2003; Biron et al. 2004). For example, Thompson et al. (2003) estimated that drag coefficient ranges from 0.0005 to 0.008 and Biron et al. Biron et al.

(2004) used a drag coefficient of 0.0025 for estimating the bed shear stress. Difficulties in estimating drag coefficient for different flow conditions are a weakness of this method (Biron et al. 2004).

2.2.4. Reynolds stress or Covariance (COV) method

Bed shear stress can be calculated from Reynolds shear stress if velocity fluctuations in the mean direction of flow and in the vertical direction of mean flow velocity are known (Kim et al. 2000; Babaeyan-Koopaei et al. 2002; Pope 2006). This can be written as:

$$\tau_0 = -\rho(\overline{u'w'}) \quad (9)$$

where u' is the velocity fluctuation (m/s) in the mean direction of flow, w' is the velocity fluctuation (m/s) in the vertical direction of mean flow velocity, and the bar denotes the average of the product of $u'$and w'over time. Highly sensitive and precise velocity measuring instruments (e.g. Acoustic Doppler Velocimeter) are required to measure the velocity fluctuations in various directions of flow (Kim et al. 2000).

2.2.5. Turbulent Kinetic Energy (TKE) method

Bed shear stress can be estimated using turbulent kinetic energy (Kim et al. 2000) and it can be written as:

$$\tau_0 = \frac{1}{2} C_1 \rho(\overline{u'^2} + \overline{v'^2} + \overline{w'^2}) \quad (10)$$

where u', v', w' are velocity fluctuations (m/s) from the mean (e.g., $u' = u - \bar{u}$) in Cartesian directions and C_1 is a coefficient, which can be taken as 0.19 or 0.2 (Kim et al. 2000; Biron et al.

2004). Like the COV method, this approach is also sensitive to velocity measuring instrument noise and flow related measuring errors (Williams and Simpson, 2004). Kim et al. (2000) suggested a modification of the TKE method where they only considered velocity fluctuation in the vertical direction.

$$\tau_0 = C_2 \rho \overline{w'^2} \quad (11)$$

where C_2 is a constant and Kim et al. (2000) suggested that their equation works best when C_2 is equal to 0.9.

2.2.6. Prandtl's seventh power (PSP) law

Prandtl (1952) has shown that velocity in the direction of flow is proportional to the seventh root of the distance from the sediment bed to the velocity measuring point. It can be written as:

$$\frac{\bar{u}}{u_*} = 8.7\left(\frac{y u_*}{\upsilon}\right)^{1/7} \quad (12)$$

where $\bar{u}$ is the velocity (m/s) in the direction of flow at a height y above the sediment bed and υ is the kinematic viscosity (m^2/s) of water. Prandtl has also shown that this approximation is true when Reynolds number is less than 1×10^5. If we assume that bed shear stress is constant throughout the sediment bed and the mixing length is not affected by the viscosity of water (Thompson et al. 2003; Liu 2006), there will be a laminar boundary layer close to the wall. So, bed shear stress can be written as:

$$\tau_o = \frac{\mu \bar{u}}{y} \quad (13)$$

where μ is the dynamic viscosity (Ns/m^2). Using equation 6 and 13, it can be written that:

$$\frac{\bar{u}}{u_*} = \frac{yu_*}{v} \tag{14}$$

If equation 14 and Prandtl's one-seventh power law (Equation 12) are solved, we obtain:

$$\tau_{wall} = 0.0228\rho(\frac{\bar{u}^7 v}{y})^{1/4} \tag{15}$$

As $\tau_{wall} = \tau_o =$ constant, bed shear stress can be estimated using equation 15 (Young and Southard 1978). Thompson et al. (2003), in their annular flume, used the PSP method and found good agreement with other methods.

We considered six critical bed shear stress estimation methods (i.e. Shields' approach, LP, PSP, TKE, RS, Kim et al. (2000)) for the analysis. As it was not possible to get accurate energy slope and drag coefficient measurements from our experimental setup, we excluded the average shear velocity method and quadratic stress law method from the research objectives.

Chapter 3: Methodology

All the experiments for testing the accuracy of the above mentioned bed shear stress theories were conducted in the Washington State University Albrook laboratory facilities. A re-circulating, low turbulence linear flume (3.66 m (12 ft) long, 0.884 m (2.9 ft) wide and 0.61 m (2.0 ft) deep) with flow provided by two 30 hp pumps was chosen for the analysis. The linear flume was modified by placing a stainless steel shear tray at the bottom of the flume. The shear tray is 1.27 m (4.16 ft) long and has the same width as the linear flume (2.9 ft). The top surface of the shear tray is at the same elevation as the bottom of the flume. The shear tray is placed over a diaphragm in such a way that the buoyancy of the diaphragm allows the shear tray to float just at the elevation of the flume bottom. A schematic of the linear flume is shown in Figure 3.1.

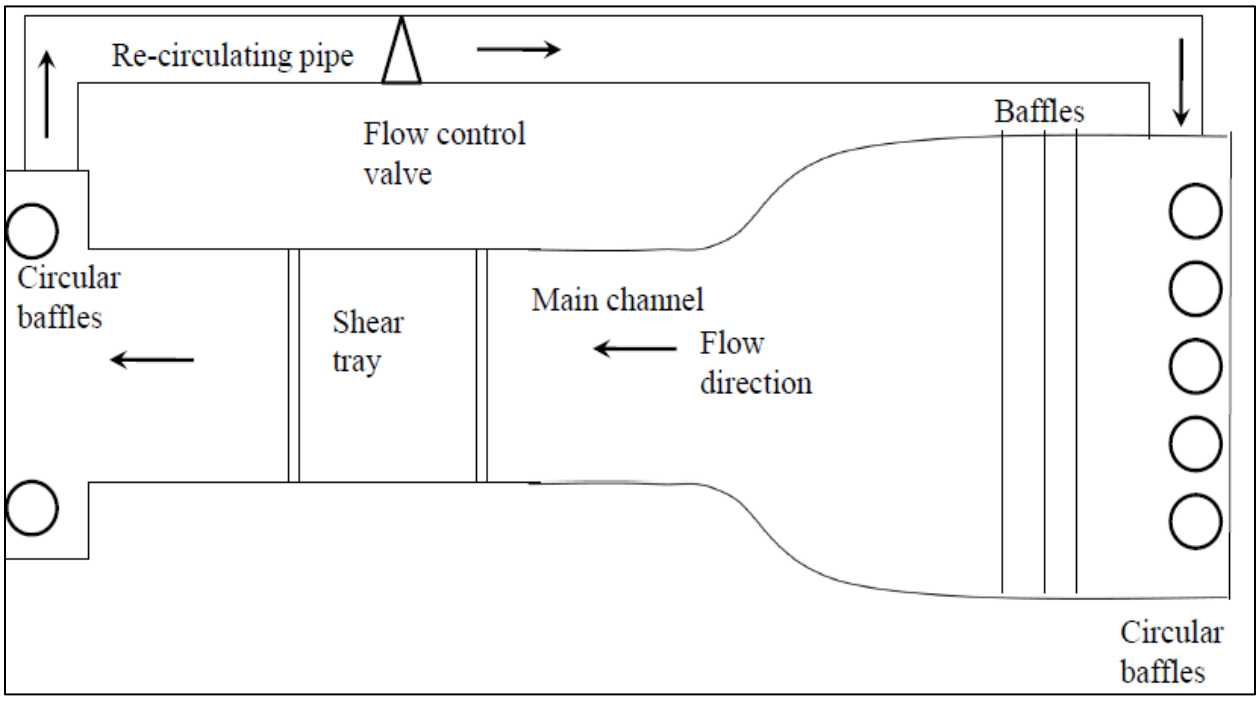

Figure 3.1 Schematic of linear low-turbulence flume.

The linear flume has two sections which are the main channel and the storage tank. The storage tank is 4.88 m (16 ft) long, 3.05 m (10 ft) wide, and 1.52 m (5 ft) deep. The storage tank is connected with the main channel by a graduating upward slope at the bottom and by two convex side walls. The re-circulating water flow into the storage tank through the re-circulating pipes. The water, in the storage tank, flow through five vertical circular baffles and three rectangular vertical baffles and enter the main channel. This setup helps reducing turbulence and creates a well developed uniform flow condition. The flow rate can be precisely controlled with the help of four valves connected to the two re-circulating pipes.

3.1. Acoustic Doppler Velocimeter (ADV)

A Nortek Acoustic Doppler Velocimeter (ADV) was used to obtain the three-dimensional velocity measurements in the flume. The ADV has the ability to take point velocity measurements and velocity fluctuations due to turbulence in the direction of Cartesian coordinates (Lohrmann et al. 1994; Kraus et al. 1994; Anderson and Lohrmann 1995; Lane et al. 1998; Voulgaris and Trowbridge 1998; Lopez and Garcia 2001). The ADV measures flow velocity using the Doppler shift principle. The ADV assumes a user defined 3-15 mm deep sampling volume which is approximately 50 mm (1.97 in) away from the transducer. The ADV sends out a beam of acoustic waves at a fixed frequency from the center transducer to the sampling volume. The reflection from moving suspended particles within the sampling volume causes a Doppler shift which is received by the 4 receivers. The ADV measures the Doppler shift of the moving particles to determine the speed of the suspended particles within the sampling volume. The ADV assumes the speed of the suspended particle equal to the flow velocity. The Nortek ADV used for this project had the ability to run at a maximum of 25 Hz frequency. We

operated the ADV at 25 Hz frequency to obtain a maximum number of velocity data in a specified time interval. The ADV probe and its operating mechanism are shown in Figure 3.2.

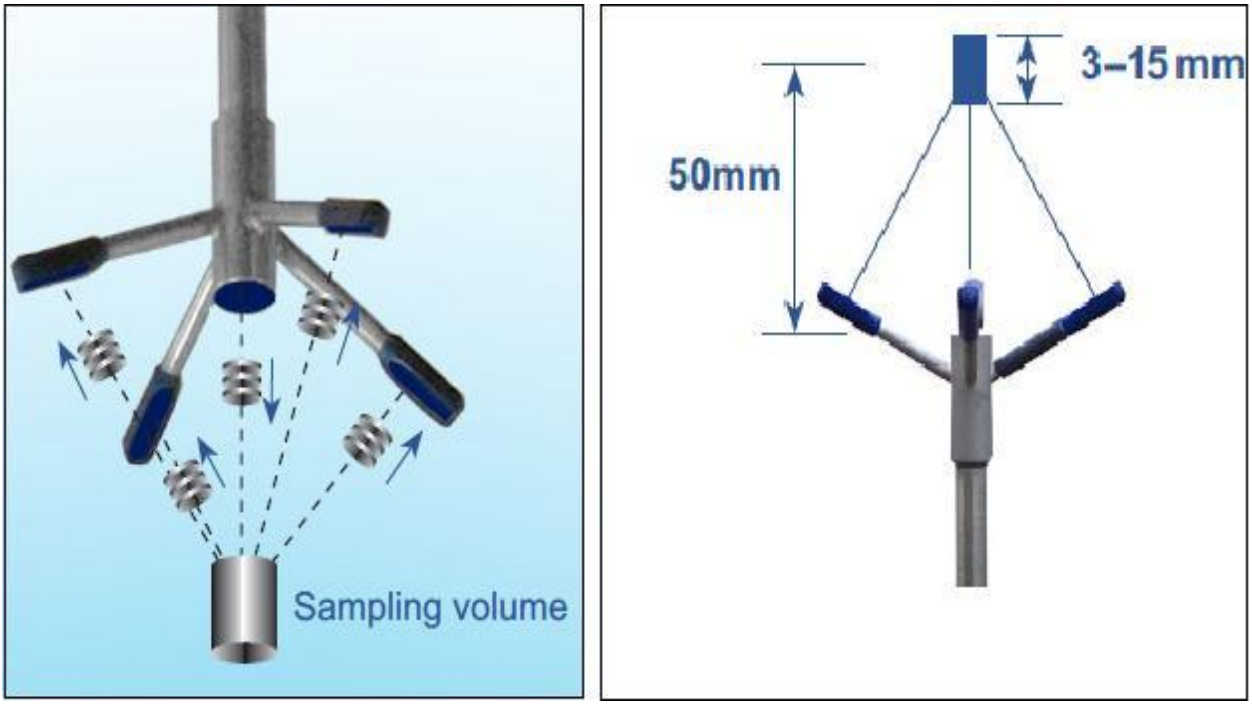

Figure 3.2 Nortek ADV probe with transducer, receiver, and sampling volume (Reproduced with permission from Nortek-US).

Though ADVs are some of the most advanced velocity measuring instruments, many researchers have expressed reservations about the turbulence measuring accuracy and sensitivity of this instrument (Voulgaris and Trowbridge 1998; Mclelland and Nicholas 2000; Goring and Nikora 2002; Barkdoll 2002). Mclelland and Nicholas (2000) suggested that measuring errors of the ADV can be controlled by the probe orientation, sampling frequency, instrument velocity range, and local flow properties. They also suggested that measurement errors could occur due to three reasons: (1) sampling errors that are hardware controlled; (2) noise that is intrinsic to the Doppler measuring technique; and (3) errors due to velocity gradient in the sampling volume.

Some errors, such as Doppler noise and velocity gradient errors, do not affect the mean velocity although they may have significant effects on the turbulence analysis such as shear stress calculation using second-order moment statistics (Lohrmann et al. 1995; Voulgaris and Trowbridge 1998). Nevertheless, ADVs have been used by several researchers (Kim et al. 2000; Thompson et al. 2003; Biron et al. 2004; Rowinski et al. 2005; Pope et al. 2006) for turbulence analysis using velocity data filtering processes suggested by Lane et al. (1998), and Goring and Nikora (2002). Despite the potential discrepancies in results, no standardized method for resolving turbulence measuring errors has been established (Rowinski et al. 2005). We ran the Nortek ADV at its maximum frequency of 25 Hz and the velocity range was maintained as close to the expected velocity as possible. This approach has been adopted as per the ADV manufacturer's suggestion and our ADV calibration observation which confirmed that the ADV measurements were accurate for our test conditions. Velocity data for the points close to the sediment bed were recorded for 4 minutes where more turbulence was expected and the rest of the data were recorded for 1 minute.

According to the Nortek user's manual, there should be a reasonable amount of suspended particles in the water for the successful operation of the ADV. We used baby powder as the seeding material to generate a sufficient number of suspended particles to facilitate measurement of the Doppler shift. We found the ADV recorded the data with an amplitude less than 60 counts and a signal correlation less than 70 when there was not any seeding materials in the flume water. The seeding materials helped to improve the amplitude to around 120 - 170 counts. The suspended particles help to obtain better sound wave reflections which eventually increase the amplitude of the instrument. Moreover, the velocity measurements with signal correlations greater than 70 were increased significantly. We found 0.5% to 15% differences in

velocities in x-direction depending on the selection of the minimum acceptable signal correlation. Figure 3.3 shows how the velocities in x-direction vary due to the different minimum acceptable signal correlation compared to no minimum signal correlation value. For example, the ADV measured a velocity of 27.87 cm/s (0.91 ft/s) if all the velocity data were retained (Velocity 1). But, the velocity was increased by 0.82% if velocity data with signal correlation under 40 was not used and it continued increasing if only the higher signal correlation values were used. Although velocities in x-direction increase as the minimum acceptable signal correlations increase, velocities in y and z directions do not follow regular trends.

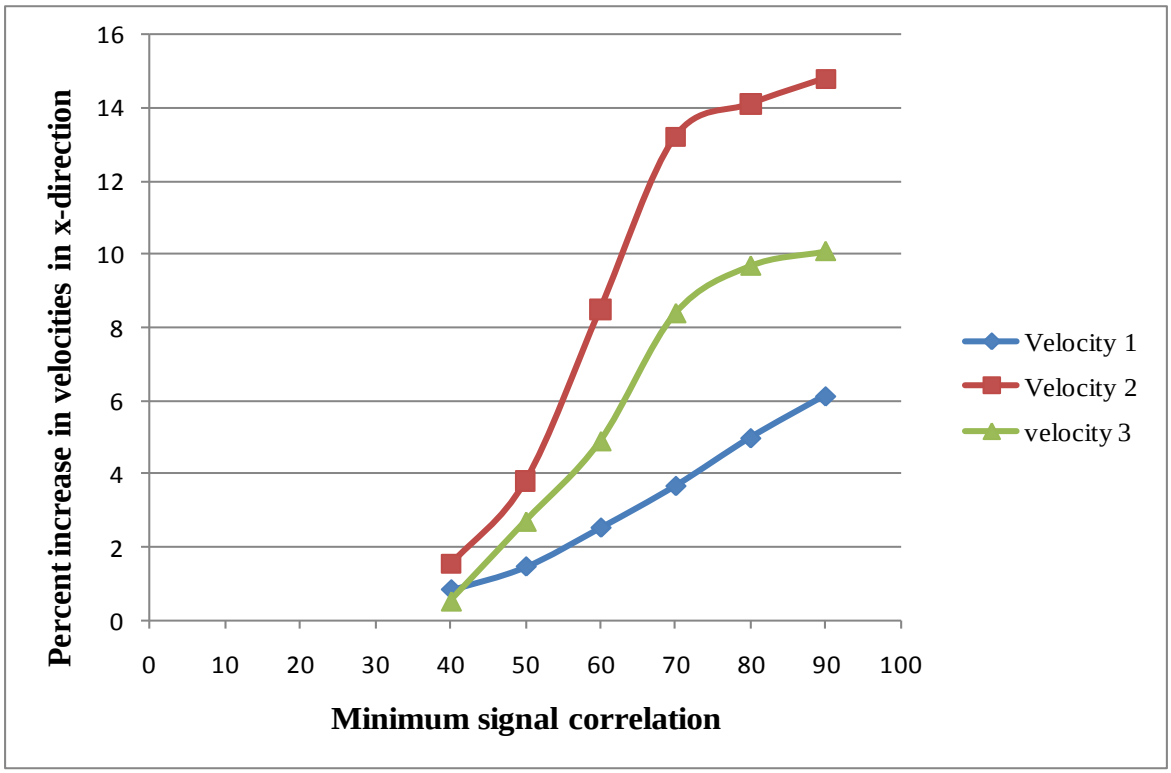

Figure 3.3 Relationship between percent change in velocities and signal correlation.

As suggested by Lane et al. (1998), ADV data with signal correlation above 70 was used for the analysis. Moreover, the amplitude was always above 100 counts. Depending on the

velocity and local flow condition, 5-30% of the data were found to generate signal correlations less than 70.

The flow velocity was increased incrementally until a visual confirmation of particle movement over the sediment bed was made. The ADV was able to record the velocity data at 0.4 cm above the sediment bed without having any interference on the sampling volume. We recorded low quality velocity data (i.e. low correlation and amplitude for most of the velocity measurements) for velocity points below 0.4 cm to the sediment bed. We recorded velocity data at 0.4 cm, 0.7 cm, 1.0 cm, 1.4 cm, and 2.0 cm to 8.0 cm with 1.0 cm increment above the sediment.

3.2. Calibration of ADV

The ADV has a very sophisticated sensor and processing unit which necessitates going through a calibration procedure to confirm all the components are in good condition. Moreover, turbulence analysis requires very high precision in velocity measurements. So, the accuracy of the ADV must be verified in addition to the manufacturer's statement of accuracy. The calibration of the ADV was performed by Angel's Instrumentation, Inc, a certified instrumentation calibration company. The calibration procedure was performed in a 5.0 m (16.4 ft) long, 1.5 m (4.92 ft) wide, and 1.5 m (4.92 ft) deep tow tank located in the Washington State University Albrook Laboratory facilities. The ADV was attached to a track, and a Stac6-Si drive motor was used to move the ADV over the track at different speeds. The tow tank was filled with water so the ADV sensor was submerged in water. The ADV was moved at different speeds with the help of the computer controlled drive motor in the still water. The calibration was made by

comparing the ADV results with the drive motor speeds. Angel's Instrumentation, Inc. confirmed the manufacturer's statement concerning the accuracy of the ADV's measurement. Calibration efforts found that the ADV velocity values to be within $\pm$ 0.5% of the measured values.

3.3. Laser Distance Meter (LDM)

In order to measure sediment movement along the test tray surface, a Keyence Model LKG-507 Laser Displacement Meter (LDM) was used. The LDM was used to obtain the uniform sediment bed profiles before flow velocities exceeded the critical value and the resulting non-uniform bed profiles after running the flume with a velocity slightly greater than the critical velocity. The goal was to produce moving dunes without visible entrainment of sediments into the water column. The LDM measures distance by triangulating the maximum intensity of the diffuse reflection from a laser beam sensor. The sensor is connected to a controller/processor which controls/processes the data collected by the sensor. The LDM's manufacturer (Keyence) claims that it has an accuracy of less than 0.2 μm. We did not calibrate the LDM independently; however the LDM results looked satisfactory with the tape measurements. The LDM is capable measuring a surface which is 50 cm $\pm$ 25 cm (19.7 in $\pm$ 9.8 in) away from the laser beam. The LDM was placed 60 cm (23.6 in) from the sediment bed which is within the instrument's range.

The actual sediment transport rate was computed using the change in bed elevation over time from the LDM data. A 25cm strip along the shear tray, located in the middle across the flume width was chosen to analyze the sediment transport rate. Six sediment bed profiles, each at 5 cm interval along the flume width were measured by the LDM. The LDM was run over the

sediment bed by a Stac6-Si drive motor at 3 cm/s (0.1 ft/s) speed. The drive motor operation was controlled by Si-programmer software supplied by the manufacturer (Tolomatic). The LDM data were recorded and processed by the LK-Navigator software supplied by the Keyence Corporation. The LDM recorded around 23000 sediment bed elevation points over a distance of 1.27 m (4.17 ft).

Sediment transport rate equations proposed by Engelund and Hansen (1967) and Ackers and White (1973) were used to determine the bed shear stress. These results were compared with the bed shear stress calculated from the previously mentioned equations.

3.4. Preparation of sediment bed

We used five different sizes of sand particles, each with a specific density of around 2.65, as the sediment bed. We followed ASTM standard sieve analysis procedures (C 136) to prepare these different sizes of sand particles. The sieve analysis was performed in the geotechnical laboratory at the Washington State University. Moreover, we followed ASTM D854 standard procedure to confirm the specific density of the sand particle. We found that the specific density of the sand particles matched with the manufacturer's statement (Specific density = 2.65). The particle size characteristics of these five different types of sediment are described in Table 3.1.

Table 3.1 Physical test sand properties.

Name of the sand type	Passed through (Sieve # - Opening in mm)	Retained at (Sieve # - Opening in mm)	Nominal size (mm)
A	20 - 0.850	25 - 0.710	0.780
B	25 - 0.710	40 - 0.425	0.567
C	40 - 0.425	50 - 0.300	0.360
D	60 – 0.250	80 – 0.180	0.215
E	100 – 0.150	200 – 0.075	0.113

In addition, six different types of sediment mixtures were used to analyze how the critical shear stress and critical velocity change compare to uniform sand. Type A and Type C sands were mixed at three different proportions to prepare three sediment mixtures. Additionally, Type B and Type D sands were mixed at three different proportions to prepare three more sediment mixtures. The detailed configuration of these sediment mixtures are tabulated in Table 3.2.

Table 3.2 Configuration of sediment mixture.

Name of the mixture type	Percentage – Sand type	Percentage – Sand type	Mixing method
M1	50 - A	50 – C	Thorough mixing by hand for 10 minutes
M2	75 - A	25 – C	
M3	25 - A	75 – C	
M4	50 - B	50 – D	
M5	75 - B	25 – D	
M6	25 - B	75 – D	

The flume was filled with water to a depth of 0.3048 m (1.0 ft) and the sand was placed over the shear tray. The sediment bed was initially laid to a uniform depth of 0.47 cm (3/16 inches) for all experiments. A screed was used to obtain a uniform sediment bed. A complete test setup is shown in Figure 3.4. Once small waves caused by the movement of the screed during the uniform sediment bed preparation process were dissipated, the pump was turned on. A valve was used to increase the flow velocity at low rates. We waited for five minutes after each incremental increase in flow velocity to check whether the critical condition occurred. Once the critical condition was observed, velocity data were recorded using the ADV.

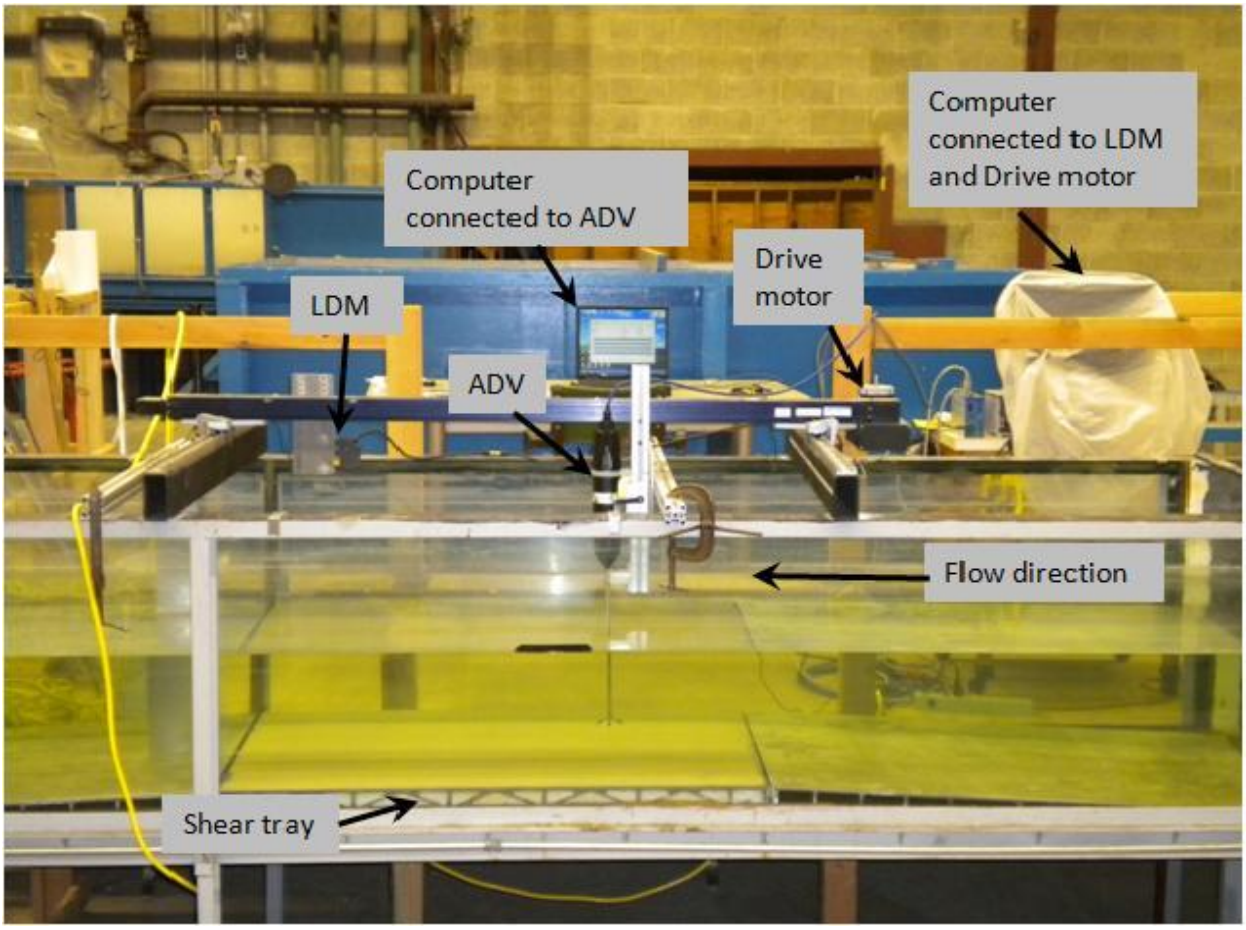

Figure 3.4 A complete test set up showing ADV, Drive motor, LDM, and sediment bed.

Chapter 4: Results

We performed five replicate experiments for each type of sand particle. The average of these five experiments was used for comparison and contrasting discussions. We observed a distinct log-layer in the bottom 2 cm of the water column for all the experiments. So, we used velocity points within the log-layer to calculate the critical bed shear stress. Current research in this field (Kim et al. 2000; Biron et al. 2004) has suggested that the velocity measurement point for estimating bed shear stress should be taken within the log-layer and as close to the sediment bed as possible. We found that velocity points above the log-layer showed almost identical velocity fluctuations for all types of sand particles at a wide range of flow velocities which confirmed the precision of current turbulence analysis practice.

Many researchers (Voulgaris and Trowbridge 1998; Kim et al. 2000; Song and Chiew 2001; Biron et al. 2004) have found higher bed shear stress at the lower portions of the log-layer compared to upper portions of the log-layer. We also found similar results and decided to use the velocity measurement points at 0.4 cm above the sediment bed to estimate the critical bed shear stress using Turbulent Kinetic Energy (TKE), Reynolds stress, and the method proposed by Kim et al. (2000). Detailed calculations of all the methods as well as the results of each experiment were tabulated and presented in Appendix 1.

4.1. Comparison among the bed shear stress estimation methods

A summary of the experimental results for uniform sand particles are shown in Table 4.1. The results showed that shear stress decreased as the particle size decreased except for the type E

sand. This trend was true for all the critical bed shear stress estimation methods except Shields' method. Shields' method was the only equation that estimated a lower shear stress value for type E sand compared to type D sand.

Table 4.1 Critical bed shear stress for different sizes of sand particles.

Sand Type	Particle Size mm	Shields' N/m^2	LP N/m^2	Prandtl N/m^2	TKE N/m^2	Reynolds N/m^2	Kim et al. N/m^2
A	0.780	0.0425	0.1147	0.2786	0.1064	0.1355	0.0455
B	0.567	0.0300	0.0927	0.2252	0.0683	0.1035	0.0419
C	0.360	0.0208	0.0655	0.1992	0.0465	0.0758	0.0346
D	0.215	0.0180	0.0358	0.1623	0.0257	0.0308	0.0112
E	0.128	0.0149	0.0591	0.1715	0.0397	0.0686	0.0298

Hjulstrom (1935) and other researchers showed that particles under around 0.2 mm diameter actually worked as a cohesive material. As a result, higher velocities are required to initiate sediment motion which eventually leads to higher critical bed shear stress values. We used sand particles ranges from 0.11 mm to 0.78 mm diameter and all the bed shear stress estimation equations except shields' approach were able to catch this behavior. Prandtl's seventh power law consistently estimated a very high critical bed shear stress for all types of sediments. The LP and Reynolds stress methods estimated consistently higher critical bed shear stress values for all sand particle sizes. Critical bed shear stresses obtained from the Shields' approach represented the smallest values predicted by any of the equations. Researchers (Vanoni 1964; Yalin and Karahan 1979; Kennedy 1995; Buffington 1999; Paphitis 2001; Pilotti and Menduni 2001) discussed problems associated with Shields' diagram and came up with a modified

Shields' diagram. As these problems have already been acknowledged by the many researchers, the problems associated with Shields' diagram will not be discussed in this paper. The method proposed by Kim et al. (2000) estimated small critical bed shear stress values compared to other methods except Shields' approach. This method estimated critical bed shear stress values from 5.6% to 50.0% higher compared to Shields' approach except for the type D sand. Surprisingly, for the type D sand, the method proposed by Kim et al. (2000) estimated critical bed shear stress value 60.7% lower compared to Shields' approach. On the other side, the method proposed by Kim et al. (2000) estimated critical bed shear stress values from 33.2% to 197.8% lower compared to the LP, TKE, and Reynolds stress methods. The graphical presentation of Table 4.1 is shown in Figure 4.1 which demonstrates how the critical bed shear stress varies with respect to particle size and the discrepancy among the five different critical bed shear stress estimation methods.

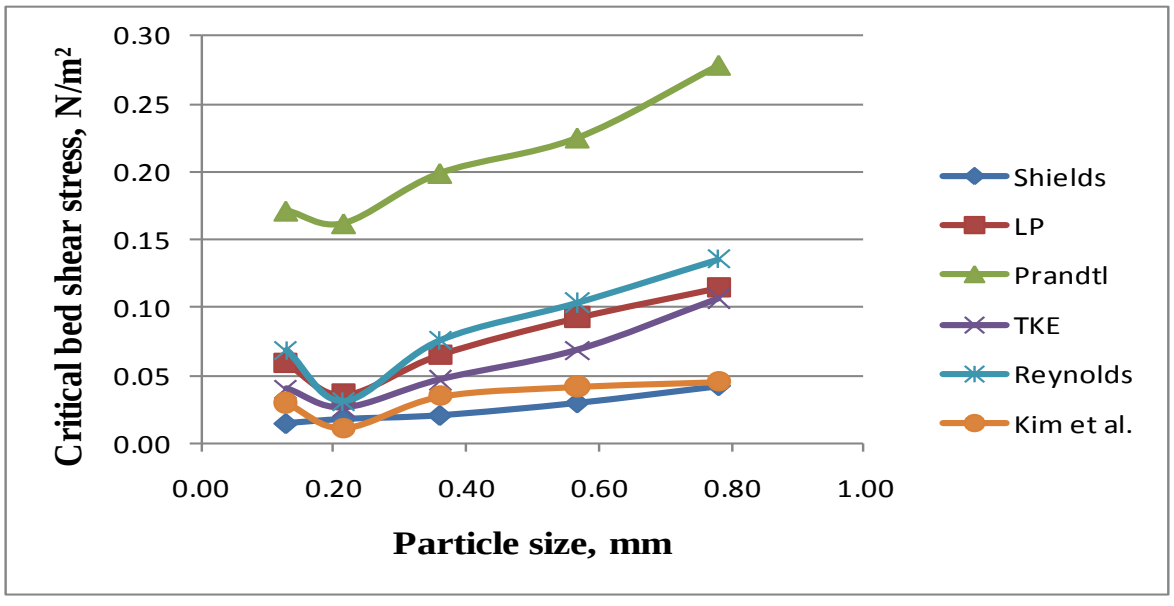

Figure 4.1 Critical bed shear stress estimated from five different methods for different sand particle sizes.

Kim et al. (2000), Biron et al. (2004), and Rowinski et al. (2005) suggested that the Reynolds stress method was one of the most accurate bed shear stress estimation methods. We compared critical bed shear stress estimates from the Reynolds stress equation with the other methods using the results of all 25 experiments for five different sizes of sand particles for the analysis. Figure 4.2 shows the comparison between Reynolds stress and other methods. Critical bed shear stress estimates from the Reynolds stress and the LP methods showed very good agreement with a slope of 0.779 and $R^2 = 0.788$. The Reynolds stress method results also showed good agreement with the values generated by TKE method, with a slope of 0.743 and $R^2 = 0.861$. But, critical bed shear stress estimates using the Reynolds stress methodology showed significant difference with the method proposed by Kim et al. (2000), with a slope of only 0.322 and $R^2 = 0.790$.

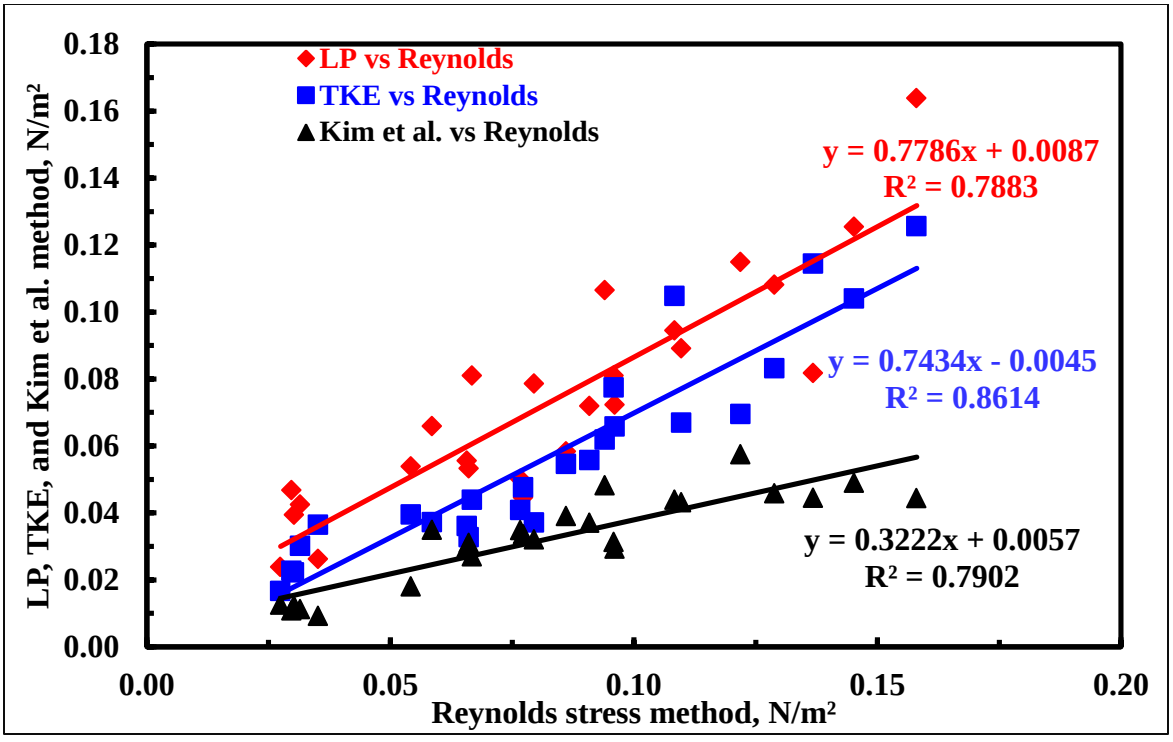

Figure 4.2 Comparison of Reynolds stress with LP, TKE, and Kim et al. methods.

4.2. Relationship between critical bed shear stress and average flow velocity

We also tried to obtain a relationship between critical bed shear stress and average flow velocity. As mentioned before, larger particles required higher average velocity and higher critical bed shear stress to initiate sediment motion. Moreover, particles below 0.2 mm in diameter required higher velocity and higher critical bed shear stress to initiate sediment motion. The critical bed shear stresses for particles larger than 0.2 mm were plotted against the average flow velocity to initiate the sediment motion (Figure 4.3). The LP, TKE, and Shields' methods showed a linear relationship between critical bed shear stress and average flow velocity, with R^2 = 0.975, R^2 = 0.991, and R^2 = 0.944, respectively. On the other hand, the Reynolds stress and Kim et al. (2000) methods also showed a linear relationship with a lower R^2 value of 0.882 and 0.824, respectively.

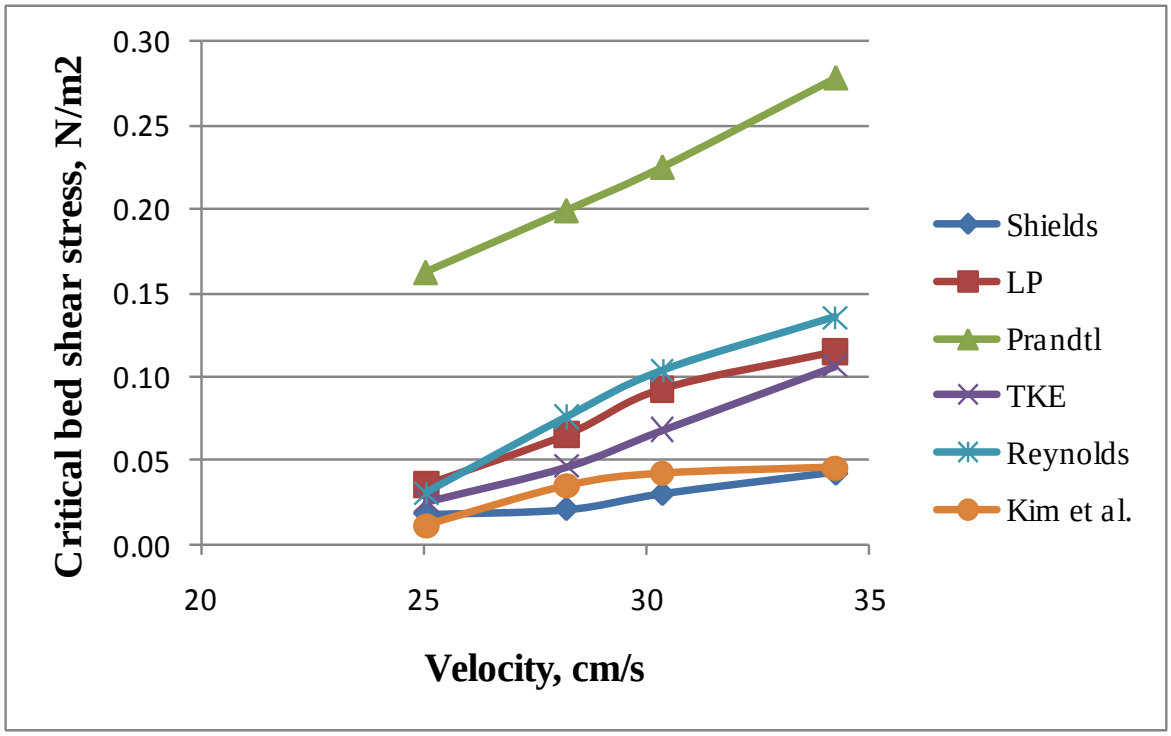

Figure 4.3 Relationship between critical bed shear stress and average flow velocity.

4.3. Comparison of bed shear stress estimation methods with sediment transport rate estimation approaches

We also compared these bed shear stress estimation methods to two widely used sediment transport rate equations (i.e. Ackers and White's formula, and Engelund and Hansen's formula). Bed shear stress can be back-calculated for a known sediment transport rate. The Laser Displacement Meter (LDM) measured the change in sediment bed elevation after running the flume for a certain amount of time. A typical sediment bed profile recorded by the LDM is shown Figure 4.4. The figure showed that there were higher sediment erosion volumes at the beginning of the tray and less erosion at the downstream end of the sediment tray. The likely cause of this was the formation of the upstream dunes which deflect water velocity at the bed surface away from the downstream sediments. The sediment transport rate was calculated using the amount of sediment eroded from the shear tray.

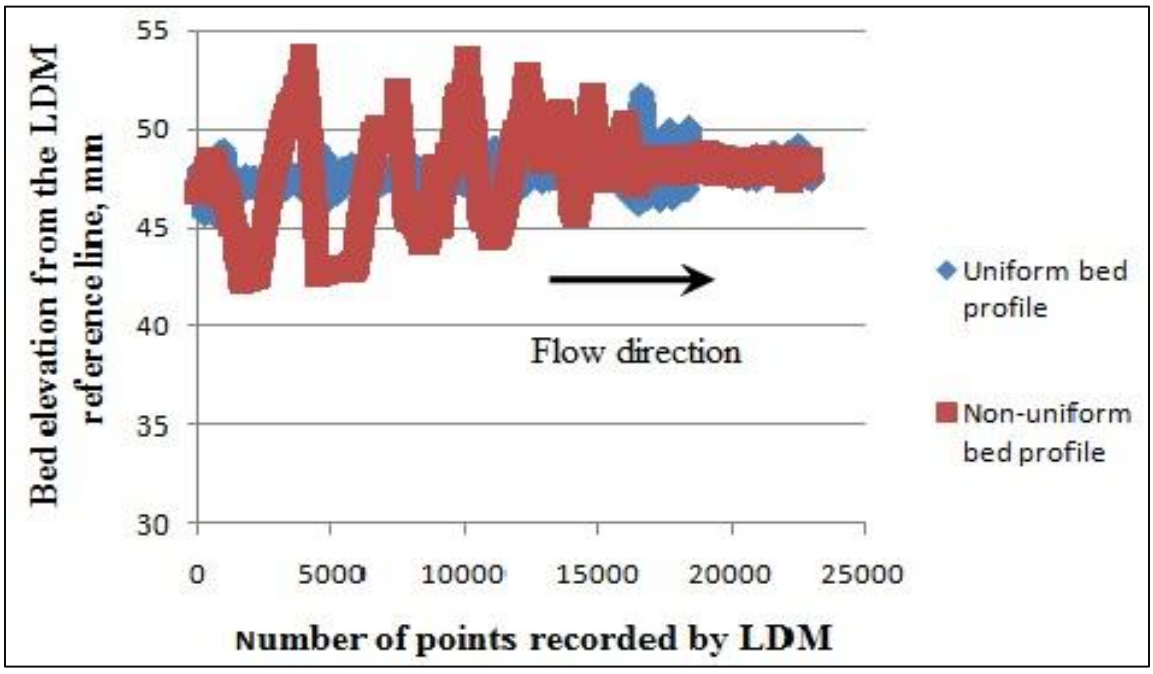

Figure 4.4 Change in sediment bed elevation for type C sand measured by LDM.

Depending on the sizes of the sand, different types of sediment bed profiles were formed due to the shear stress exerted by the water on the sediment bed. A sediment bed profile with dunes and ripples formed in type C sand. On the other hand, irregular scouring pattern throughout the sediment beds were observed for other types of sands. The bed forms for different types of sediments are shown in Figure 4.5. Theoretically, the total bed shear stress would be the sum of the skin stress acting on the sediment particles and form stress produced by the type of bed forms such as dunes and ripples (Kostaschuk et al. 2004). This means that the type of bed form plays an important role in the bed shear stress estimations.

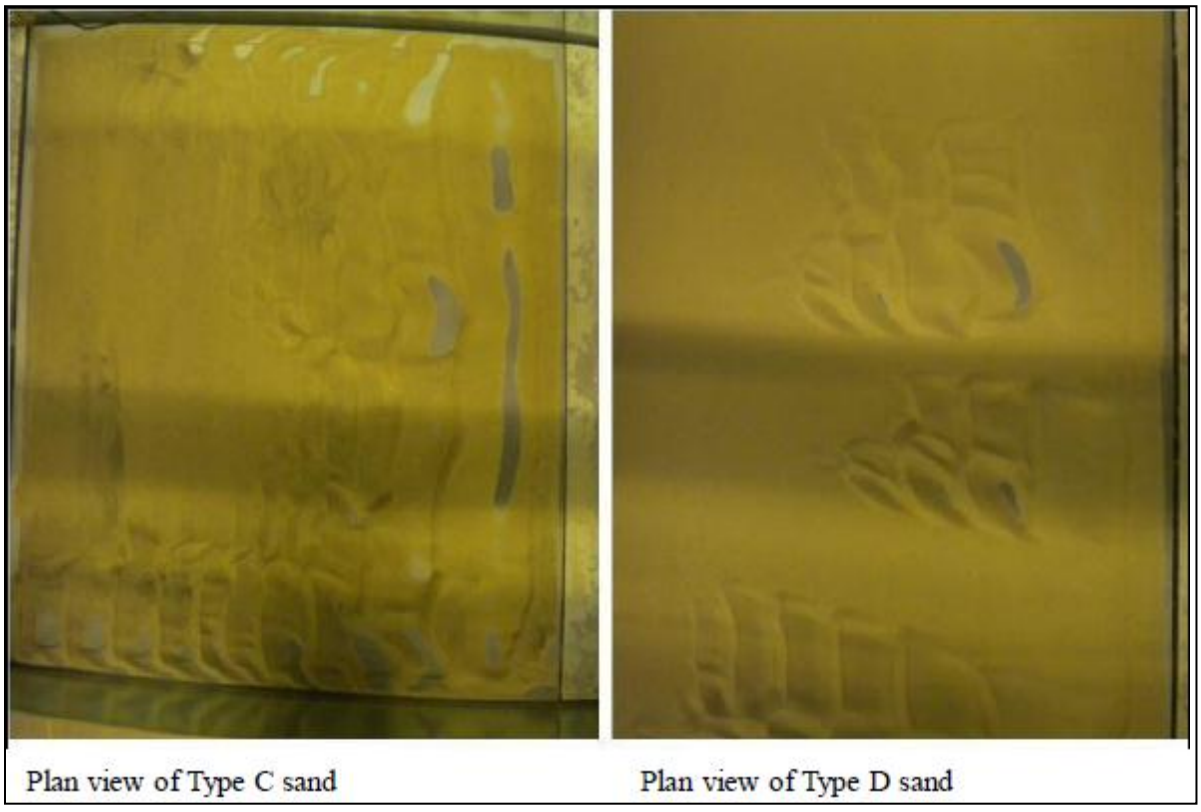

Figure 4.5 Sediment bed Plan views for the type C and D sands.

The measured sediment transport rate and corresponding bed shear stress values from different methods are shown in Table 4.2. The Prandtl's seventh power law estimated a very high bed shear stress value compared to the other bed shear stress estimation methods. The LP method also estimated high bed shear stress values for all types of sands. The bed shear stress calculated from the two sediment transport rate methods showed a significant difference. The Ackers and White's method estimated a very high bed shear stress value for the measured sediment transport rate. This means that Ackers and White equation underestimated the rate of sediment transport under this type of flow condition. Bisantino et al. (2010) also found that Ackers and White equation underestimated sediment transport during the long-term application. On the other hand, bed shear stress estimated from Engelund and Hansen's method showed considerable agreement with the different types of bed shear stress estimation methods. The method proposed by Kim et al. (2000) estimated very small bed shear stress values for all types of sediments which were very similar to our critical bed shear stress test results.

Table 4.2 Comparing the bed shear stress estimation equations with sediment transport estimation approaches.

Sand Type	Particle Size, mm	Engelund and Hansen, N/m^2	Ackers and White, N/m^2	LP N/m^2	Prandtl N/m^2	TKE N/m^2	Reynolds N/m^2	Kim et al. N/m^2
A	0.780	0.1850	1.8250	0.2238	0.2652	0.1306	0.1682	0.0599
B	0.567	0.2300	1.4440	0.1700	0.2256	0.0952	0.1204	0.0466
C	0.360	0.1108	0.6503	0.3014	0.1935	0.0992	0.1411	0.0691
D	0.215	0.0956	0.6605	0.0846	0.1532	0.0708	0.0942	0.0425
E	0.128	0.0755	0.5476	0.1291	0.1620	0.0853	0.1031	0.0439

Bed shear stress estimated from the measured sediment transport rate could be regarded as the pseudo measured bed shear stress and Engelund and Hansen's method appeared to be more applicable than Ackers and White's method for our experimental flow conditions. So, we compared bed shear stress estimated from LP, TKE, Reynolds stress, and Kim et al. (2000) methods with the pseudo measured bed shear stress estimated from Engelund and Hansen's method. The analysis is shown in figure 4.6.

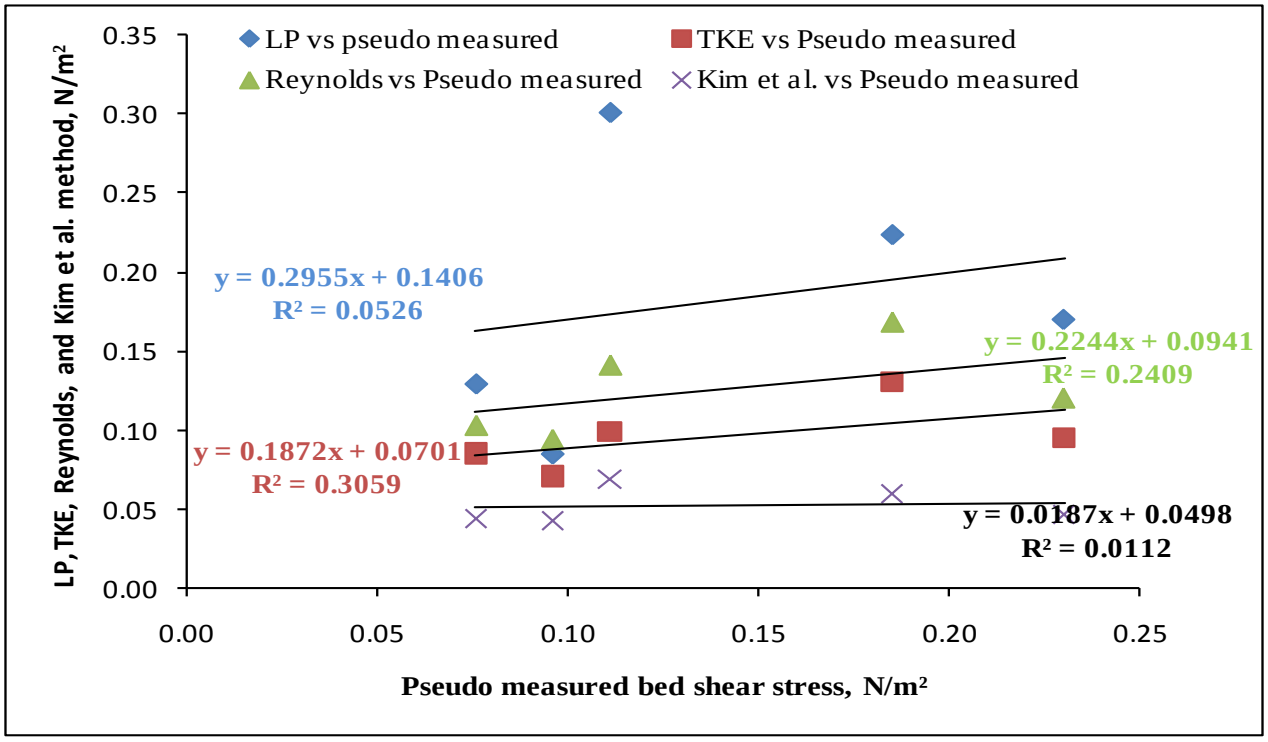

Figure 4.6 Comparison of pseudo measured value with LP, TKE, Reynolds and Kim et al. methods.

Bed shear stress estimates from the LP method and pseudo measured bed shear agreed with a slope of 0.296 and R^2 = 0.053. The Reynolds stress method results agreed with the pseudo measured value generated by Engelund and Hansen's method, with a slope of 0.224 and R^2 = 0.241. The TKE method showed similar agreement with a slope of 0.187 and R^2 = 0.306. But,

bed shear stress estimates using method proposed by Kim et al. (2000) showed significant difference with the pseudo measured value, with a slope of only 0.0.019 and $R^2 = 0.011$. In addition, higher discrepancies were observed among the LP, TKE, and Reynolds stress results for sediment transport than critical condition.

4.4. Comparison of critical bed shear stress between different sizes of sediment beds and sediment mixture beds

One of the main objectives of our research was to find how the critical bed shear stress of a mixture of different types of sand varied compared with sediment beds of individual sand types used in the sediment mixture. The results for this investigation are tabulated in Table 4.3.

Table 4.3 Critical bed shear stresses for different sizes of sediment beds and different mixtures of sediment beds.

Sand Type	LP N/m^2	Prandtl N/m^2	TKE N/m^2	Reynolds N/m^2	Kim et al. N/m^2	Average velocity cm/s
A	0.1147	0.2786	0.1064	0.1355	0.0455	34.24
C	0.0655	0.1992	0.0465	0.0758	0.0346	28.21
M1	0.1764	0.2784	0.1038	0.1359	0.0441	34.39
M2	0.1534	0.2671	0.0824	0.1266	0.0425	33.73
M3	0.0730	0.2013	0.0545	0.0762	0.0357	28.27
B	0.0927	0.2252	0.0683	0.1035	0.0419	30.36
D	0.0358	0.1623	0.0257	0.0308	0.0112	25.06
M4	0.1020	0.2339	0.0710	0.0774	0.0287	30.88
M5	0.0821	0.2279	0.0548	0.0612	0.0165	30.32
M6	0.0386	0.1599	0.0278	0.0420	0.0171	24.95

Sediment mixture types M1, M2, and M3 were prepared by using a different percentage of type A and type C sand. Sediment mixture types M4, M5, and M6 were prepared by using percentages of type B and type D sand. The details of the sediment mixtures were described in the sediment preparation section. Two graphs were plotted for a better understanding of the variation in critical bed shear stresses for sediment bed mixtures. These graphs are shown in Figure 4.7 and Figure 4.8. We found maximum critical bed shear stresses for sediment mixtures prepared with 50% of the type A and C sands (M1) and 50% of the type B and type D sands (M4). Type M2 and M5 sediment beds (i.e., 75% of larger sand particles and 25% of smaller sand particles) showed similar critical bed shear stresses of sediment beds prepared only by larger particle present in the sediment mixtures. On the other hand, type M3 and M6 sediment beds (i.e., 25% of larger sand particles and 75% of smaller sand particles) showed critical bed shear stress values similar to those produced by the beds only having the smaller particle present in the sediment mixtures. The average flow velocities required to initiate sediment motion were higher for the type M1 and M4 sediment beds. Moreover, the average flow velocities required for initiation of motion for type M2, M3, M5, and M6 sediment beds showed similar results closely relating to the dominant particle size in the system.

LP method estimated 10.03% to 53.82% increase in bed shear stresses for sediment beds with equal amount of both types of sands (i.e., M1 and M4) compared to sediment beds prepared only by largest particle size present in the sediment mixture bed. On the other hand, Prandtl, TKE, Reynolds, and Kim et al. (2000) estimated -0.07% to 3.86%, -2.41% to 3.88%, -25.22% to 0.30%, and -3.01% to -31.48% change respectively for similar condition. LP method estimated -11.43% to 11.45% change in bed shear stresses for sediment beds with 75% of one type and 25%

of another type of sands (i.e., M2, M3, M5, and M6) compared to sediment beds prepared only by dominant particle size present in the sediment mixture bed. On the other hand, Prandtl, TKE, Reynolds, and Kim et al. (2000) estimated -4.12% to 1.20%, -22.56% to 17.25%, -40.87% to 36.36%, and -60.54% to 51.96% change respectively for similar condition. So, responses from the different bed shear estimation equations due to sand size distribution in the sediment beds were different.

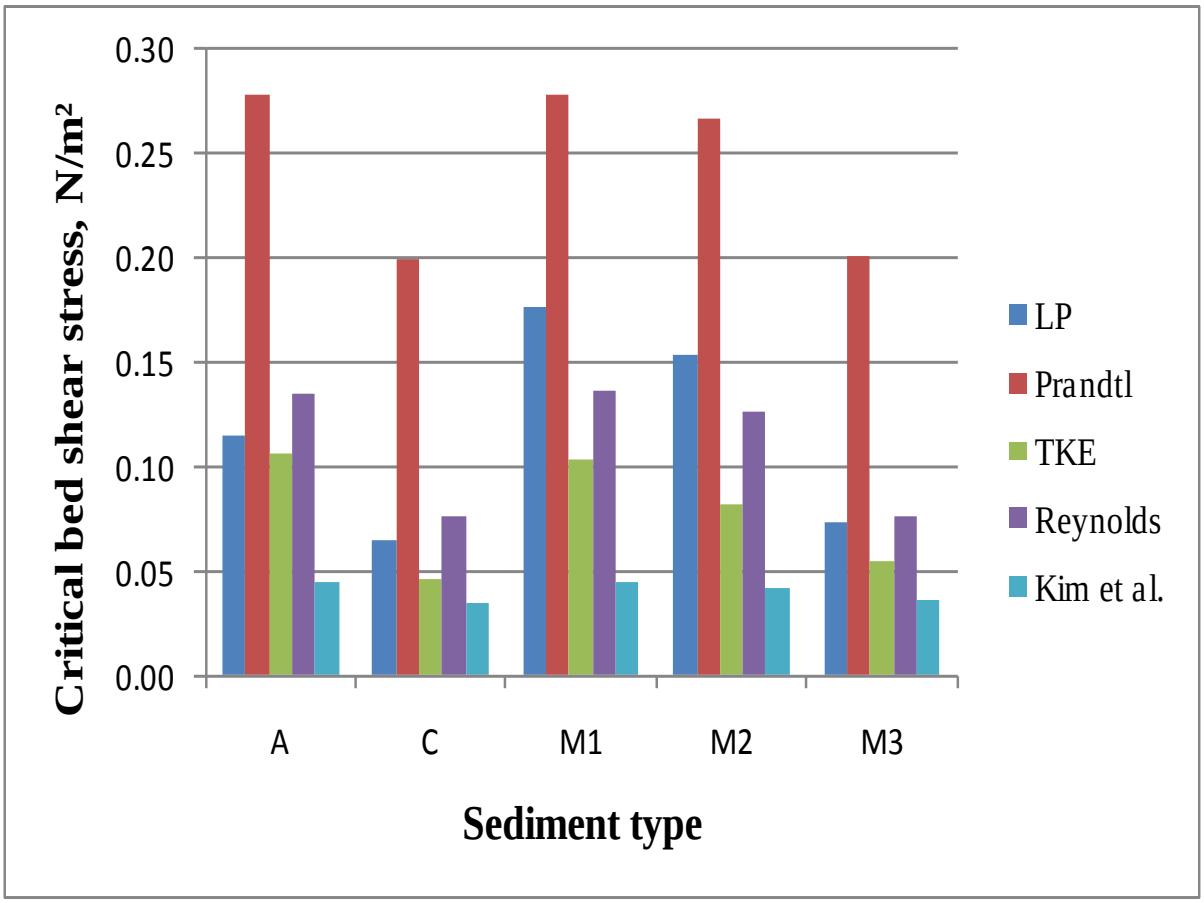

Figure 4. 7 Comparison of critical bed shear stress of type A and type C sands with sediment mixtures prepared using different percentages type A and type C sands.

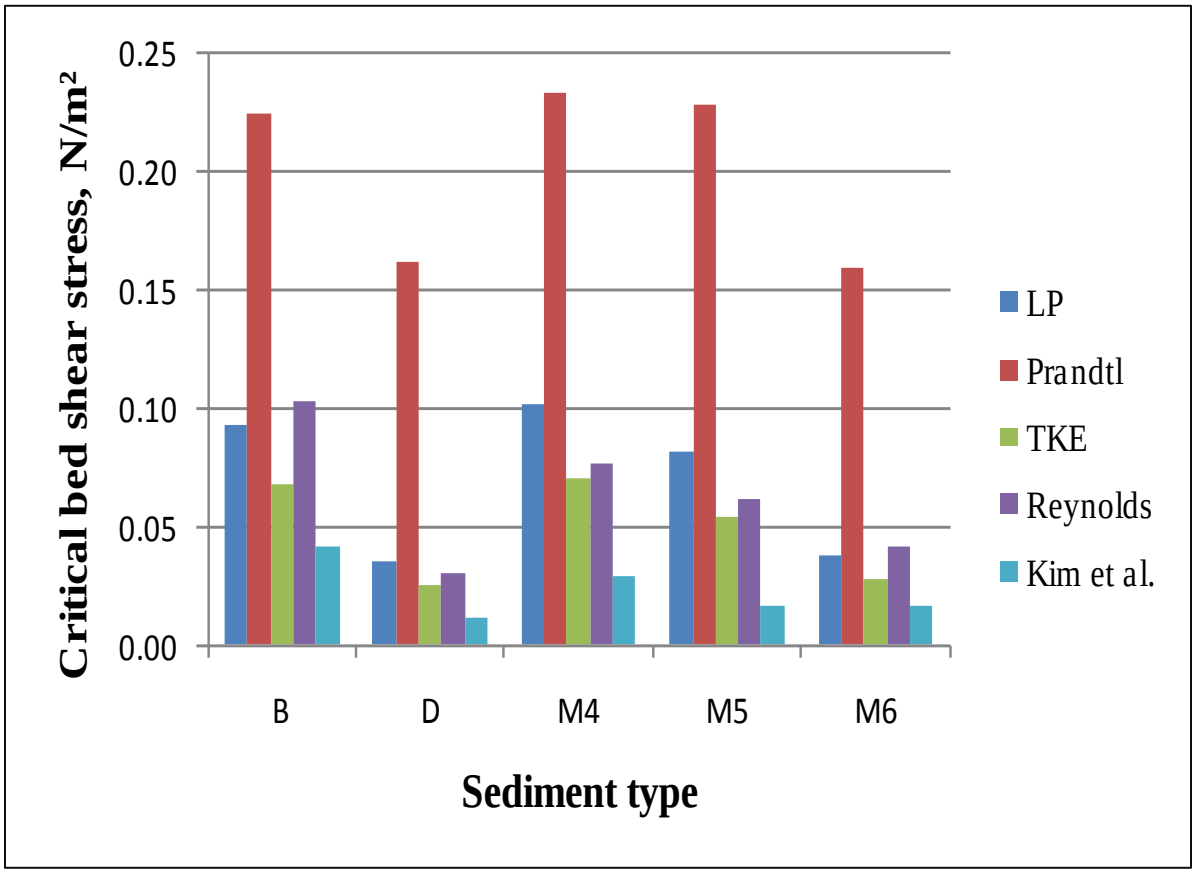

Figure 4. 8 Comparison of critical bed shear stress of type B and type D sands with sediment mixtures prepared using different percentages type B and type D sands.

4.5. Importance of selecting velocity data point for the turbulence based bed shear stress methods

As mentioned earlier, the ADV was able to record velocity data below 0.4 cm of the sediment bed (e.g., 0.1 cm, 0.2 cm etc.) with low correlation and low amplitude values. However, 10% to 25% velocity measurement values were found to be within acceptable correlation and amplitude range for those velocity measuring points. The bed shear stresses

measured from these acceptable velocity measurement values for different types of sediment beds did not show consistent results in terms of replicating the results for same flow condition. So, for the present experimental set up and flow conditions, it was not possible to record high quality velocity measurement values with the ADV for velocity data points 0.4 cm below the sediment bed.

The bed shear stress could have been measured using velocity data points at 0.7 cm, or 1.0 cm above the sediment bed. Some bed shear stress sample calculations were made to understand how the bed shear stress varies due to the different velocity point selection. As expected, bed shear stresses calculated using velocity data of those points (i.e., 0.7 cm and 1.0 cm above sediment bed) were consistently lower than the bed shear stresses calculated using the velocity data of 0.4 cm above the sediment bed.

Chapter 5: Discussions

For all the experiments, a distinct log-layer around 2.0 cm (0.79 in) thick was found adjacent to the sediment bed. We used five velocity points within the log-layer to estimate the bed shear stress using the LP method. As a result, we did not have enough velocity points to have significant confidence in the LP method estimations. However, the LP method showed significant agreement with Reynolds stress method for different particle sizes of sediment beds. Conversely, the LP method showed consistently higher values of bed shear stress for the sediment mixture beds. Kim et al. (2000) and Biron et al. (2004), in their study, found consistently higher bed shear stresses estimated by the LP method. Aberle et al. (2003) suggested that higher bed shear stress values were due to not having a fully developed boundary layer. Moreover, Rowinski et al. (2005) suggested that the LP method should not be used for very shallow depths. Our experimental set up was developed in such a way that a fully developed boundary layer could occur in the region near the shear tray. We also used a flow depth of 30.48 cm (1.0 ft) which is not very shallow. Consequently, flow conditions in our experimental setup produced reasonable bed shear stress values compared to other researchers' results. However, a deeper log-layer with more velocity points within the log-layer would have been better to get bed shear stresses with higher confidence limits.

Prandtl's seventh power law estimated the highest bed shear stresses for all types of sediment beds. Thompson et al. (2003), in their 0.4 m (1.31 ft) deep annular flume, found that Prandtl's seventh power law estimated bed shear stresses in good agreement with other methods. Thompson et al. (2003) also found a distinct log-layer of around 2.0 cm (0.79 inch) in their annular flume set up. We found similar velocities for the points above the log-layer in all the

experiments. It made the Prandtl's seventh power law difficult to implement, because this method uses an equation with velocity and flow depth. So, the same velocity with a different flow depth will estimate a different bed shear stress. More specific methods to choose the velocity points need to be investigated for the successful implementation of the Prandtl's seventh power law.

The LP method and the Prandtl's seventh power law are dependent upon accurate velocity and depth measurements with a fully developed boundary layer. But, this is not necessarily the case in a natural flow field (Aberle et al. 2003; Thompson et al. 2003). Bed shear stress estimation by turbulence measurements is a better option for any flow condition (Kim et al. 2000; Aberle et al. 2003; Thompson et al. 2003; Biron et al. 2004; Rowinski et al. 2005). Turbulence measurement based bed shear stress estimation methods such as the TKE method, the Reynolds stress method, and the method proposed by Kim et al. (2000) showed consistent results for all types of sediment beds. The Reynolds stress method estimated the highest values and the method proposed by Kim et al. (2000) estimated lowest bed shear stress among these three methods. So, turbulence measurement based bed shear stress estimation methods can be used to reliably estimate the bed shear stress for a wide range of bed roughness. Biron et al. (2004) and Rowinski et al. (2005) suggested that the Reynolds stress method would give a better result for a simple steady, uniform flow field. On the other hand, Kim et al. (2000) suggested that both TKE and Reynolds stress methods would give better results if near bed turbulence measurements were available. We found that bed shear stress estimated from the TKE and Reynolds stress methods showed considerable agreement for different types of sediment beds. Moreover, the bed shear stress estimated from the sediment transport rate estimation methods such as Engelund and Hansen method showed considerable agreement with the TKE and

Reynolds stress methods. The method proposed by Kim et al. (200) estimated very small values of bed shear stress for all types of sediment beds. Figure 5 and Figure 6 clearly indicated the differences between Kim et al. (2000) and other methods. This method is only based on the velocity fluctuations in the vertical direction of flow which are usually lower than streamwise velocity fluctuations and across the flow (i.e. along the width of the channel) velocity fluctuations. Kim et al. (2000) proposed their bed shear stress estimation method to reduce instrument noise errors as noise errors due to vertical velocity fluctuations are smaller than streamwise velocity fluctuations and velocity fluctuations along the width of the channel (Voulgaris and Trowbridge 1998). However, the Kim et al. (2000) method needs to be revisited as we found a significant difference in bed shear stress with other methods for the simple steady uniform flow condition.

Thompson et al. (2003) developed a relationship between bed shear stress and average flow velocity or velocity at a certain depth. We also found a similar type of relationship for critical bed shear stress with average flow velocity. However, developing a standard relationship between bed shear stress and average flow velocity would be very difficult as the bed shear stress would be different for different flow conditions and structures of the dunes and ripples formed due to the sediment movement from the bed.

Most previous flume experiments, with some exceptions such as Wiberg and Smith (1987), Kuhnle (1993), and Shvidchenko et al. (2001), to estimate bed shear stress in the past years were performed using smooth sediment beds with uniform particle sizes. We performed a set of experiments with mixed sediment beds prepared by mixing different sizes of particles. These experiments allowed us to investigate how the bed shear stress varied with different

mixture of sediment beds. It was expected that sediment beds with different sizes of particles would be difficult to move compared to sediment beds of individual particle size because the void spaces between larger particles will be filled with smaller particles which would eventually result in compact sediment beds. We found that sediment beds with different sizes of sand particles tended to develop a bed shear stress similar to sediment beds with the dominant particle size in the mixed sediment beds. Moreover, if a sediment bed is prepared with equal amounts of different sizes of particles, the bed shear stress tended to be similar to the sediment bed prepared by the largest particle size in the mixed sediment bed. So, we have to be very careful to describe a mixed sediment bed with a representative individual particle size. In addition, comparison of different bed shear stress estimation equations under sediment bed prepared by mixture of different sizes sands seemed to be more complicated. Because, the change in bed shear stresses due to sediment bed mixtures were varying with a wide range for different bed shear stress estimation equations. That means, agreement among the different bed shear stress estimation equations vary due to the sediment bed mixtures compared to sediment bed prepared by uniform sands.

We used velocity point at 0.4 cm (0.1575 inches) above the sediment bed for the turbulence measurements. Others researchers have suggested using velocity points at 10% of the boundary layer thickness or 0.1 of the flow depth or at some other depths (Kim et al. 2000; Biron et al. 2004). We found that 0.4 cm (0.1575 inches) above the sediment bed was the closest near sediment bed velocity point with good quality velocity measurements data. Moreover, other velocity data points such as 0.7 cm or 1.0 cm could have been used for the bed shear stress measurements which would estimate a lower shear stress values compared to velocity data point 0.4 cm (0.1575 inches) above the sediment bed. A consistency for the selection of velocity point

among the researchers to perform turbulence measurements would be very helpful to achieve a better agreement.

All the velocity, turbulence, and sediment transport rate measurements for this study were done by currently available most advanced techniques. Though ADV is one of the most advanced velocity measurement instruments, more research requires to reduce instrument noise and to simplify the data recording procedures.

Chapter 6: Conclusions

Fifty sediment scour experiments were performed using five cohesionless sediment sizes classified as sand to get an idea about the relative accuracy of six widely-used bed shear stress estimation methods. As expected, our critical velocity results for all of the sediment sizes showed good agreement with the Hjulstrom's diagram. Using LDM measurements of scour rates and both the Ackers and White and Engelund and Hansen equations, surrogate values for "actual" bed shear stresses were determined and compared with the six widely-used methods to determine the validity of these approaches for sand sediment scour problems. Actual bed shear stresses back-calculated from the measured sediment transport rate were different for the Ackers and White and Engelund and Hansen equations.

First, using a uniform sand size (defined as sand being retained on a single sieve), critical bed shear stress estimation by LP, TKE, and Reynolds stress methods showed good agreement for sediment beds prepared using uniform sands. But, the discrepancies among the bed shear stress equations were higher for sediment transport conditions compared to critical conditions. That means, agreement among the bed shear stress estimation methods were less when sediment bed is in transport condition. Moreover, Shields, PSP, and Kim et al. (2000) showed more discrepancies for both critical and sediment transport conditions.

Second, bed shear stresses back-calculated from LDM measured sediment transport rates using both Ackers and White and Engelund and Hansen methods also confirmed the relative acceptability (i.e., slope of 0.187 to 0.224 and R^2 = 0.241 to 0.306) of both TKE and Reynolds stress methods compared to the other methods (i.e., slope of 0.019 to 0.296 and R^2 = 0.011 to

0.053). However, all the bed shear stress estimation methods are subject to different types of errors such as instrument noise errors, selection of velocity point above the sediment bed for the turbulence analysis, instrument misalignment errors, Doppler noise due to the increased shear within the sampling volume, and absence of a constant stress layer (Kim et al. 2000; Thompson et al. 2003; Biron et al. 2004; Rowinski et al. 2005). So, whenever possible, several methods should be used to get an idea about the possible range of the bed shear stress and for different types of sediment beds and flow conditions. In addition, current research results can be used to select the appropriate shear stress estimation methods for that particular local flow environment. We should also be focused on the laboratory flume experiments based accurate direct bed shear stress measurements so that these bed shear stress estimation methods could easily be re-evaluated by comparing with the direct bed shear stress measurements.

Bed shear stresses estimated from measured sediment transport rates using Ackers and White's method showed large discrepancies with all the bed shear stress estimation methods for this flow condition. Bed shear stresses estimated from measured sediment transport rates using Engelund and Hansen's method showed considerably better agreement with most of the bed shear stress estimation methods. In some cases (i.e., TKE and RS method results for type B sand, and LP method result for type C sand), however, the Engelund and Hansen method also showed large discrepancies (92% to 172%).

For the third objective, we found that sediment beds with different sizes of sands produced similar or higher bed shear stress compared to sediment beds prepared with dominant particle present in the mixture. Sediment beds prepared with equal amount of two sand types showed maximum critical bed shear stress compared to sediment beds prepared with mixing the

sands in different proportions or sediment beds prepared with uniform size sands. Sediment beds prepared with 75% of one type sand and 25% of another type sand tended to produce similar critical bed shear stresses compared to sediment beds prepared with only the dominant particle size present in the mixture. Moreover, discrepancies among the bed shear stress estimation equations were higher which confirmed that applicability of these equations varied under sediment beds with different sizes of sands. This investigation has been performed for six sediment beds prepared by mixing two different sand types. More experiments with sediment beds prepared by three and more different sand types are required to achieve concrete idea about the behavior of sediment bed with mixed sands.

Reference List

Aberle, J. and Smart, G. M. (2003). "The influence of roughness structure on flow on steep slopes." *J. Hydr. Res.*, 41(5), 259-269.

Ackers, P. and White, W. R. (1973). "Sediment transport: New approach and analysis." *J. Hydr. Div., ASCE,* 99(11), 2041-2060.

Ahmed, F. and Rajratnam, N. (1998). "Flow around bridge piers." *J. Hydr. Engrg., ASCE,* 124(3), 288-300.

Aksoy, H. and Kavvas, M. L. (2005). "A review of hillslope and watershed scale erosion and sediment transport models." *Catena,* 64, 247-271.

Anderson, S., and Lohrmann, A. (1995). "Open water test of the Sontek acoustic Doppler velocimeter." *Proc., IEEE Fifth Working Conf. on Current Measurements*, IEEE Oceanic Engineering Society, St. Petersburg, Fla., 188–192.

Babaeyan-Koopaei, K., Ervine, D. A., Carling, P. A., and Cao, Z. (2002). "Velocity and turbulence measurements for two overbank flow events in River Severn." *J. Hydr. Engrg., ASCE,* 128(10), 891–900.

Bagnold, R. A. (1966). "An approach to the sediment transport problem from general physics." *U. S. Geological Survey Professional Paper 422-1.*

Barkdoll, B. (2002). "Discussion of 'Mean flow and turbulence structure of open-channel flow through non-emergent vegetation,' by F. Lopez, and M. H. García." *J. Hydr. Engrg., ASCE,* 128(11), 1032.

Barnes, M. P., O'Donoghue, T., Alsina, J. M., and Baldock, T. E. (2009). "Direct bed shear stress measurements in bore-driven swash." *Coastal Engineering*., 56(8), 853-867.

Bathurst, J. C. (1982). "Theoretical aspects of flow resistance in gravel-bed Rivers, edited by R. D. Hey, J. C. Bathurst, and C. R. Thorne." 83-105, John Wiley, NY.

Beheshti, A. A.,and Ataie-Ashtiani, B. (2008). "Analysis of threshold and incipient conditions for sediment movement." *Coastal Engineering*, 55 (3), 423–430.

Biron, P. M., Lane, S. N., Roy, A. G., Bradbrook, K. F., and Richards K. S. (1998). "Sensitivity of bed shear stress estimated from vertical velocity profiles: The problem of sampling resolution." *Earth Surface Processes and landforms*, 23, 133-140.

Biron, P. M., Robson, C., Lapointe, M. F., and Guskin, S. J. (2004). "Comparing different methods of bed shear Stress estimates in simple and complex flow fields." *Earth Surface Processes and Landforms*, 29, 1403-1415.

Bisantino, T., Gentilee, F., Milella, P., and Liuzzi, G. T. (2010). "Effect of time scale on the performance of different sediment transport formulas in a semiarid region." *J. Hydr. Engrg., ASCE,* 136(1), 56-61.

Bridge, J. S. and Jarvis, J. (1976). "Flow and sedimentary processes in the meandering River South Esk, Glen Clova, Scotland." *Earth Surface Processes and landforms*, 1, 303-336.

Bridge, J. S. and Jarvis, J. (1976). "Velocity profiles and bed shear stress over various bed configurations in a river bend." *Earth Surface Processes and landforms*, 2, 281-294.

Buffington, J.M. and Montgomery, D.R. (1997). "A systematic analysis of eight decades of incipient motion studies, with special reference to gravel-bedded rivers." *Water Resour. Res.*, 33(8), 1993-2029.

Buffington, J. M. (1999). "The legend of A. F. Shields." *J. Hydr. Engrg, ASCE,* 125(4), 376-387.

Cui, Y. and Parker, G. (2005). "Numerical model of sediment pulses and sediment-supply disturbances in mountain rivers." *J. Hydr. Engrg., ASCE,* 131(8), 646-656.
Engelund, F. and Hansen, E. (1967). "A monograph on sediment transport in alluvial streams." *Teknish Forlag, Technical Press, Copenhagen, Denmark.*
Ferguson, R. I., Ashmore, P. E., Ashworth, P. J., Paola, C., and Prestegaard, K. L. (1989). "Influence of sand on hydraulics and gravel transport in a braided gravel bed river." *Water Resour. Res.*, 25(4), 635-643.
Goring, D. G., and Nikora, V. I. (2002). "Despiking Acoustic Doppler Velocimeter data." *J. Hydr. Engrg., ASCE*, 128(1), 117–126.
Gust, G. (1988). "Skin Friction Probes for Field Applications." *J. Geophys. Res*., 93, 14121-14132.
Guy, H. P., Simons, D. B., and Richardson, E. V (1966). "Summary of alluvial channel data from flume experiment, 1956- 1961." *U. S. Geological Survey Professional Paper 462-1.*
Hjulstrom, F. (1935). "Studies of the morphological activity of rivers as illustrated by the River Fyris." *Bulletin of the Geological Institution of the University of Upsala*, Chapter 3, 292-343.
Kim, S-C, Friedrichs, C.T., Maa, JP-Y, Wright, L.D. (2000). "Estimating bottom stress in tidal boundary layer from Acoustic Doppler velocimeter data." *J. Hydr. Engrg., ASCE,* 126(6), 399–406.
Kostaschuk, R., Villard, P., and Best, J. (2004). **"**Measuring velocity and shear stress over dunes with Acoustic Doppler Profiler." *J. Hydr. Engrg., ASCE*, 130(9), 932-936.
Kraus, N. C., Lohrmann, A., and Cabrera, R. (1994). "New Acoustic Meter for Measuring 3D Laboratory Flows." *J. Hydr. Engrg., ASCE,* 120(3), 406-412.
Krishnappan, B. G., and Engel, P. (2004). "Distribution of Bed Shear Stress in Rotating Circular Flume." *J. Hydr. Engrg., ASCE*, 130(4), 324-331.
Kuhnle, R. A. (1993). "Incipient motion of sand/gravel sediment mixtures." *J. Hydr. Engrg., ASCE,* 119(12), 1400–1415.
Lamb, M. P., Dietrich, W. E., and Venditti, J. G. (2008). "Is the critical Shields stress for incipient sediment motion dependent on channel-bed slope?" *J. Geophys. Res.*, 113(5), F02008.
Lane, S., et al. (1998). "Three-dimensional measurement of river channel flow processes using acoustic Doppler velocimetry." *Earth Surf. Processes Landforms*, 23, 1247–1267.
Lau, Y. L. and Engel, P. (1999). "Inception of sediment transport on steep slopes." *J. Hydr. Engrg., ASCE,* 125(5), 544–547.
Ling, C. (1995). "Criteria for incipient motion of spherical sediment particles." *J. Hydr. Engrg., ASCE,* 121(6), 472–478.
Liu, P. L. –F. (2006). "Turbulent boundary-layer effects on transient wave propagation in shallow water*." Proceedings of the Royal Society A*, 462, 3481-3491.
Lohrmann, A., Cabrera, R., and Kraus, N. C. (1994). ''Acoustic-Doppler velocimeter (ADV) for laboratory use.'' *Fundamentals and advancements in hydraulic measurements and experimental proceedings, ASCE,* Reston, Va., 351–365.
Lohrmann, A., Cabrera, R., Gelfenbaum, G., and Haines, J. (1995). ''Direct measurements of Reynolds stress with an acoustic Doppler velocimeter.'' *Proc., IEEE 5th Working Conf. on Current Measurement,* IEEE, Piscataway, N.J., 205–210
Lopez, F., and Garcia, M. H. (2001). "Mean flow and turbulence structure of open-channel flow through nonemergent vegetation." *J. Hydr. Engrg., ASCE*, 127(5), 392–402.

McLelland, S., and Nicholas, A. (2000). "A new method for evaluating errors in high-frequency ADV measurements." *Hydrolog. Process.*, 14, 351–366.
Mehta, A. J. and Lee, S. (1994). "Problem in linking the threshold condition for the cohesionless and cohesive sediment grain." *J. Coastal Res*., 10(1), 170-177.
Molinas, A., and Wu, B. (2001). "Transport of sediment in large sand-bed rivers." *J. of Hydr. Res*., 39(2), 135-146.
Nezu, I., and Nakagawa, H. (1993). *Turbulence in open channel flows*, IAHR, Balkema, Rotterdam, The Netherlands.
Papanicolaou, A. N., Diplas, P. Evaggelopoulos, N., and Fotopoulos, S. (2002). "Stochastic incipient motion criterion for spheres under various bed packing conditions." *J. Hydr. Engrg., ASCE*, 128(4), 369-380.
Paphitis, D. (2001). "Sediment movement under unidirectional flows: an assessment of empirical threshold curves." *Coastal Engineering* 43(5), 227–245.
Pilotti, M., and Menduni, G. (2001). "Beginning of sediment transport of incoherent grains in shallow shear flows." *J. Hydr. Res*., 39(2), 115-124.
Pope, N. D., Widdows, J., and Brinsley, V. (2006). "Estimation of bed shear stress using the Turbulent Kinetic Energy approach—A comparison of annular flume and field data." *Continental Shelf Res*., 26(4), 959-970.
Prandtl, L. (1952). Essentials of fluid dynamics, Blackie & sons, London, UK.
Rankin, K. L., and Hires, R. I. (2000). "Laboratory measurement of bottom shear stress on a movable bed." *J. Geophys. Res*., 105, 17011-17019.
Rowinski, P. M., Aberle, J., and Mazurczyk, A. (2005). "Shear velocity estimation in hydraulic research." *Acta Geophysica Polonica*, 53(4), 567-583.
Shvidchenko, A. B., Pender, G., and Hoey, T. B. (2001). "Critical shear stress for incipient motion of sand/gravel streambeds." *Water Resour. Res*., 37(8), 2273-2283.
Song, T. and Chiew, Y. M. (2001). "Turbulence measurement in nonuniform open-channel flow using Acoustic Doppler Velocimeter (ADV)." *J. Engrg. Mech., ASCE*, 127(3), 219-232.
Thompson, C. E. L., Amos, C. L., Jones, T. E. R., and Chaplin, J. (2003). "The manifestation of fluid-transmitted bed shear stress in a smooth annular flume – A comparison of methods." *J. Coastal Res*., 19(4), 1094-1103.
Vanoni, V. A. (1964). "Measurement of critical shear stresses for entraining fine sediments in a boundary layer." *Final Report to U. S. Public Health Service Research Grant RG-69 15*, Report No. KH-R-7, May 1964.
Voulgaris, G., and Trowbridge, J. (1998). "Evaluation of the Acoustic Doppler Velocimeter (ADV) for turbulence measurements." *J. Atmos. Ocean. Technol.*, 15(1), 272–288.
Westenbroek, S. M. (2006). "Estimates of shear stress and measurements of water levels in the Lower Fox River near Green Bay, Wisconsin." *USGS Scientific Investigations Report*, 2006-5226.
White, C. M. (1940). "The Equilibrium of Grains on the Bed of a Stream." *Royal Society of London. Series A, Mathematical and Physical Sciences*, 174(2), 322-338.
Wiberg, P. L., and Smith, J. D. (1987). "Calculations of the critical shear stress for motion of uniform and heterogeneous sediments." *Water Resour. Res*., 23(8), 1471-1480.
Wilcock, P. R. and Southard, J. B. (1988). "Experimental study of incipient motion in mixed-size sediment." *Water Resour. Res.*, 24(7), 1137-1151.

Wilcock, P. R. (1996). "Estimating local bed shear stress from velocity observations." *Water Resour. Res.*, 32(11), 3361–3366.
Wilcock, P. R. (2001). "Toward a practical method for estimating sediment-transport rates in gravel-bed Rivers." *Earth Surf. Process. Landforms* 26, 1395–1408.
Wilcock, P. R., and Crowe, J. C. (2003). "Surface-based transport model for mixed-size sediment." *J. Hydr. Engrg., ASCE*, 129(2), 120-128.
Williams, E., and Simpson, J. H. (2004). "Uncertainties in estimates of Reynolds stress and TKE production rate using the ADCP variance method*." J. Atmospheric and Oceanic Technology*, 21 (2), 347-357.
Wolf, J. (1999). "The estimation of shear stresses from near-bed turbulent velocities for combined wave-current flows*." Coastal Engineering*, 37, 529–543.
Wu, C. and Chou, Y. (2003). "Rolling and lifting probabilities for sediment entrainment." *J. Hydr. Engrg., ASCE*, 129(2), 110-119.
Yalin, M. S. and Karahan, E. (1979). "Inception of sediment transport." *J. Hydr. Div.*, 105(11), 1433-1443.
Yang, C. T. (1977). "The Movement of Sediment in Rivers." *Geophysical Surveys* 3, 39-68.
You, Z. J., and Yin, B. S. (2007). "Direct measurement of bottom shear stress under water waves." *J. Coastal Res.*, 50, 1132-1136.
Young, R. N. and Southard, J. B. (1978). "Erosion of fine-grained marine sediments: Sea-floor and laboratory experiments." *Geophysical Society of American Bulletin*, 89(5), 663-672.

Appendix 1

Bed shear stress calculation using Shields' approach

Value of $\frac{d}{\upsilon}[0.1\left(\frac{\gamma_s}{\gamma}-1\right)gd]^{0.5}$ was calculated for each type of sediment and dimensionless shear stress parameter ($\frac{\tau_0}{(\gamma_s-\gamma)d}$) was predicted from the Shields' diagram. Bed shear stress calculated from the predicted dimensionless shear stress parameter.

Bed shear stress calculation using LP method

Equation 1, $\frac{u}{u_*}=\frac{1}{K}\ln(\frac{z}{z_0})$ can be written as:

$u = m(lnz) + c$, where $m=\frac{u_*}{K}$ and $c = u_*(lnz_0)$. Velocities at different depths (z) were plotted against lnz and critical velocities were calculated using slope (m) of the graph. Bed shear stress was calculated using equation 2 ($\tau_0 = \rho u_*^2$).

Test results for Type A sand

Run	Sand size, mm	Shields' N/m^2	Hjulstrom cm/s	Observed cm/s	LP N/m^2	Prandtl N/m^2	TKE N/m^2	Reynolds N/m^2	Kim et al. N/m^2
1	0.780	0.0425	17-35	33.93	0.1082	0.2763	0.0832	0.1288	0.0459
2	0.780	0.0425	17-36	34.62	0.1254	0.2865	0.1041	0.1452	0.0490
3	0.780	0.0425	17-37	34.63	0.0945	0.2851	0.1047	0.1084	0.0439
4	0.780	0.0425	17-38	34.61	0.0817	0.2836	0.1144	0.1369	0.0445
5	0.780	0.0425	17-38	33.43	0.1638	0.2614	0.1256	0.1581	0.0444
Average				34.24	0.1147	0.2786	0.1064	0.1355	0.0455

Test results for Type B sand

Run	Sand size, mm	Shields' N/m^2	Hjulstrom cm/s	Observed cm/s	LP N/m^2	Prandtl N/m^2	TKE N/m^2	Reynolds N/m^2	Kim et al. N/m^2
1	0.567	0.0300	14-30	30.93	0.0719	0.2245	0.0658	0.0961	0.0293
2	0.567	0.0300	14-30	30.05	0.0891	0.2231	0.0669	0.1097	0.0431
3	0.567	0.0300	14-30	29.97	0.1065	0.2225	0.0619	0.0941	0.0482
4	0.567	0.0300	14-30	30.26	0.1149	0.2251	0.0696	0.1219	0.0575
5	0.567	0.0300	14-30	30.61	0.0810	0.2307	0.0775	0.0959	0.0313
Average				30.36	0.0927	0.2252	0.0683	0.1035	0.0419

Test results for Type C sand

Run	Sand size, mm	Shields' N/m^2	Hjulstrom cm/s	Observed cm/s	LP N/m^2	Prandtl N/m^2	TKE N/m^2	Reynolds N/m^2	Kim et al. N/m^2
1	0.360	0.0208	15-25	28.10	0.0719	0.1986	0.0557	0.0909	0.0370
2	0.360	0.0208	15-25	28.19	0.0659	0.2002	0.0372	0.0586	0.0349
3	0.360	0.0208	15-25	28.35	0.0810	0.1986	0.0439	0.0668	0.0270
4	0.360	0.0208	15-25	27.98	0.0501	0.1964	0.0409	0.0767	0.0348
5	0.360	0.0208	15-25	28.43	0.0584	0.2022	0.0546	0.0861	0.0390
Average				28.21	0.0655	0.1992	0.0465	0.0758	0.0346

Test results for Type D sand

Run	Sand size, mm	Shields' N/m^2	Hjulstrom cm/s	Observed cm/s	LP N/m^2	Prandtl N/m^2	TKE N/m^2	Reynolds N/m^2	Kim et al. N/m^2
1	0.215	0.0180	15-25	25.07	0.0468	0.1605	0.0227	0.0297	0.0109
2	0.215	0.0180	15-25	24.86	0.0242	0.1605	0.0167	0.0274	0.0126
3	0.215	0.0180	15-25	24.91	0.0394	0.1607	0.0222	0.0303	0.0123
4	0.215	0.0180	15-25	25.3	0.0262	0.1643	0.0365	0.0352	0.0093
5	0.215	0.0180	15-25	25.18	0.0425	0.1655	0.0302	0.0315	0.0112
Average				25.06	0.0358	0.1623	0.0257	0.0308	0.0112

Test results for Type E sand

Run	Sand size, mm	Shields' N/m^2	Hjulstrom cm/s	Observed cm/s	LP N/m^2	Prandtl N/m^2	TKE N/m^2	Reynolds N/m^2	Kim et al. N/m^2
1	0.128	0.0149	18-30	25.81	0.0560	0.1698	0.0410	0.0542	0.0187
2	0.128	0.0149	18-30	25.69	0.0817	0.1700	0.0386	0.0795	0.0334
3	0.128	0.0149	18-30	25.75	0.0554	0.1707	0.0340	0.0661	0.0322
4	0.128	0.0149	18-30	25.74	0.0578	0.1706	0.0374	0.0657	0.0309
5	0.128	0.0149	18-31	26.3	0.0446	0.1766	0.0476	0.0773	0.0336
Average				25.86	0.0591	0.1715	0.0397	0.0686	0.0298

Test results for Type M1 sediment mixture

Run	Sand size, mm	Shields' N/m^2	Hjulstrom cm/s	Observed cm/s	LP N/m^2	Prandtl N/m^2	TKE N/m^2	Reynolds N/m^2	Kim et al. N/m^2
1	0.78 and 0.36	N/A	17-35	34.2	0.2016	0.2780	0.1336	0.1652	0.0547
2	0.78 and 0.36	N/A	17-35	34.1	0.1971	0.2784	0.1130	0.1485	0.0439
3	0.78 and 0.36	N/A	17-35	34.63	0.1608	0.2787	0.0954	0.1152	0.0343
4	0.78 and 0.36	N/A	17-35	34.61	0.1459	0.2786	0.0734	0.1147	0.0437
Average				34.39	0.1764	0.2784	0.1038	0.1359	0.0441

Test results for Type M2 sediment mixture

Run	Sand size, mm	Shields' N/m^2	Hjulstrom cm/s	Observed cm/s	LP N/m^2	Prandtl N/m^2	TKE N/m^2	Reynolds N/m^2	Kim et al. N/m^2
1	0.78 and 0.36	N/A	17-35	32.83	0.2132	0.2549	0.0792	0.1048	0.0310
2	0.78 and 0.36	N/A	17-35	33.991	0.1721	0.2774	0.0911	0.1461	0.0504
3	0.78 and 0.36	N/A	17-35	33.5	0.1201	0.2596	0.0761	0.1265	0.0427
4	0.78 and 0.36	N/A	17-35	34.61	0.1082	0.2764	0.0832	0.1288	0.0459
Average				33.73	0.1534	0.2671	0.0824	0.1266	0.0425

Test results for Type M3 sediment mixture

Run	Sand size, mm	Shields' N/m^2	Hjulstrom cm/s	Observed cm/s	LP N/m^2	Prandtl N/m^2	TKE N/m^2	Reynolds N/m^2	Kim et al. N/m^2
1	0.78 and 0.36	N/A	17-35	28.66	0.0733	0.2085	0.0605	0.0935	0.0396
2	0.78 and 0.36	N/A	17-35	28.35	0.0578	0.2013	0.0542	0.0830	0.0372
3	0.78 and 0.36	N/A	17-35	27.98	0.0884	0.1970	0.0536	0.0632	0.0337
4	0.78 and 0.36	N/A	17-35	28.07	0.0726	0.1982	0.0496	0.0649	0.0325
Average				28.27	0.0730	0.2013	0.0545	0.0762	0.0357

Test results for Type M4 sediment mixture

Run	Sand size, mm	Shields' N/m^2	Hjulstrom cm/s	Observed cm/s	LP N/m^2	Prandtl N/m^2	TKE N/m^2	Reynolds N/m^2	Kim et al. N/m^2
1	0.567 and 0.215	N/A	N/A	30.84	0.0640	0.2348	0.0668	0.0618	0.0202
2	0.567 and 0.215	N/A	N/A	30.91	0.0774	0.2351	0.0782	0.0928	0.0489
3	0.567 and 0.215	N/A	N/A	30.89	0.1237	0.2336	0.0692	0.0640	0.0154
4	0.567 and 0.215	N/A	N/A	30.86	0.1430	0.2320	0.0697	0.0912	0.0304
Average				30.88	0.1020	0.2339	0.0710	0.0774	0.0287

Test results for Type M5 sediment mixture

Run	Sand size, mm	Shields' N/m^2	Hjulstrom cm/s	Observed cm/s	LP N/m^2	Prandtl N/m^2	TKE N/m^2	Reynolds N/m^2	Kim et al. N/m^2
1	0.567 and 0.215	N/A	N/A	30.34	0.0404	0.2274	0.0523	0.0524	0.0127
2	0.567 and 0.215	N/A	N/A	30.28	0.0968	0.2280	0.0497	0.0588	0.0180
3	0.567 and 0.215	N/A	N/A	30.31	0.0953	0.2280	0.0583	0.0675	0.0188
4	0.567 and 0.215	N/A	N/A	30.33	0.0960	0.2283	0.0587	0.0662	0.0167
Average				30.32	0.0821	0.2279	0.0548	0.0612	0.0165

Test results for Type M6 sediment mixture

Run	Sand size, mm	Shields' N/m^2	Hjulstrom cm/s	Observed cm/s	LP N/m^2	Prandtl N/m^2	TKE N/m^2	Reynolds N/m^2	Kim et al. N/m^2
1	0.567 and 0.215	N/A	N/A	25.03	0.0341	0.1596	0.0339	0.0479	0.0167
2	0.567 and 0.215	N/A	N/A	25.01	0.0270	0.1600	0.0227	0.0336	0.0156
3	0.567 and 0.215	N/A	N/A	24.90	0.0548	0.1594	0.0287	0.0444	0.0183
4	0.567 and 0.215	N/A	N/A	24.88	0.0384	0.1606	0.0261	0.0421	0.0177
Average				24.95	0.0386	0.1599	0.0278	0.0420	0.0171